19th World Congress of Soil Science

Symposium 1.1.2
Soil morphology and environment hazards

Soil Solutions for a Changing World,

Brisbane, Australia

1 – 6 August 2010

Table of Contents

Andic soils and catastrophic mudflows in Italy: Morphological and hydropedological evidences

Fabio Terribile [A], Michela Iamarino [A], Antonella Agrillo [A], Angelo Basile[B], Roberto De Mascellis[B], Giuliano Langella[B], Giacomo Mele[B], Antonio Mileti [A], Luciana Minieri [A], Pierpaolo Moretti [A], Simona Vingiani [A]

[A]Università di Napoli Federico II, DISSPAPA, Portici Napoli, Italy; Email; fabio.terribile@unina.it
[B]CNR ISAFOM Ercolano, Napoli, Italy, Email a.basile@isafom.cnr,it

Abstract
In Italy rapid landslides are the most frequently occurring natural disasters and, after earthquakes, cause the highest number of victims. In this contribution we attempt to prove that there exists a tight connection between the presence of a specific soil type, namely andic soils, and the occurrence of the main catastrophic mudflows and debris flows occurred in Italy in the last decades. The study was performed by means of an integrated pedological and hydrological analysis on the detachment crowns of some of the most important catastrophic mudflows and debris flows that occurred in Italy in the last decades and involving/evolving surface soils. The results at both regional (Campania) and National (Italy) scale clearly show that despite the large variability of the environmental settings of the studied sites there are indeed some striking homogeneous soil features in the detachment crowns including (i) soil morphology, (ii) andic features ranging from high to moderate, (iii) high water retention throughout a large range of pressure heads. Results seem to reveal clear cause-effect evidences between andic soils and the investigated catastrophic mudflows/debrisflows; this must be related to the unique physical properties of these soils inducing high landslide vulnerability.

Key Words
Landslide, hydropedology, andic soils

Introduction
Due to its relief and its lithological and structural characteristics, Italy is a country where landslides are the most frequently occurring natural disasters and are the cause, after earthquakes, of the highest number of victims. The national landlslide inventory database (IFFI) surveyed 482,272 landslides covering an area of almost 20,500 km^2, which is equivalent to 6.8% of Italy. In such scenario rapid mudflows (and debrisflows) are among the major catastrophic types of landslides occurring in Italy especially in terms of victims and damages. Mudflow is a very rapid to extremely rapid flow (i.e. velocity 0.05–5 m s^{-1}) of saturated plastic materials having a high water content (e.g. Hungr *et al*., 2001). Fast mudflow landslides are grave dangers to people and infrastructures as they can potentially activate large amounts of materials across extended distances in very short time periods. In this contribution we attempt to demonstrate that there is tight connection between the presence of a specific soil type, namely andic soils, and the occurrence of the main catastrophic mudflows and debrisflows occurred in Italy in the last decades and involving/evolving surface soils. In order to perform such study we performed an integrated pedological and hydrological analysis on the detachment crowns of some of the most important catastrophic mudflows and debrisflow occurred in Italy in the last decades and involving/evolving surface soils. We investigated the following landslide sites: Sarno (1998), Salerno (1954), Platì (1951), Versilia (1996) and Albaredo (1987, 2002). A more detailed hydro-pedological study was also performed, using a 2D Richard's based water balance simulation model, in order to address two critical issues for Campanian flow slides susceptibility, namely (i) the presence of discontinuities along the slope (e.g. roads, cliffs, etc.) (ii) the relationship with slope aspect. It must be emphasised that, a part from the sites of Campania (Sarno and Salerno), no andic soil are reported in the available soil maps referring to the other Italian sites.

Methods
The point based and land based integrated analysis carried out in this study focus on the only catastrophic landslides producing fast mudflows (Table 1). We selected landslides that caused human victims and have suitable technical documentation in the published literature. Landslides occurring before 1841 were not been considered. More than 20 soil profiles from 19 detachment crowns were described and analysed in the field. Only the six most representative sites are given in this contribution attempting to cover a large range of landscapes in terms of geology, geomorphology and latitude. The upper parts of slopes where detachment occurs are generally extremely steep (more than 50-60°). The profiles have been described using the FAO system (1990). Undisturbed soil samples for hydrological analysis were collected from the main horizons with steel cylinders of about 100 and 200 cm^3. Bulk soil samples were also collected from all soil horizons.

1 – 6 August 2010, Brisbane, Australia. Published on DVD.

After air drying, samples were sieved to less than 2 mm and analysed according to USDA (1996) methods: pH in H_2O, organic matter by the Walkley-Black method, Al, Fe and Si in the amorphous oxides/hydroxides and in the organic matter were selectively extracted with ammonium oxalate (Feo, Alo, Sio) treatment at pH=3 (Schwertmann, 1964) and with sodium pyrophospate (Fep, Alp, Sip) (Bascomb,1968), respectively, and their content levels were determined by ICP-AES. Values of Al and Fe extracted with ammonium oxalate were used to calculate the andic property index Alo+0.5Feo. Allophane and imogolite quantities were estimated using the Parfitt (1990) method, based on selective extractions. On undisturbed soil samples the saturated hydraulic conductivity was measured applying the constant head method (Klute and Dirksen, 1986). Following an evaporation process, the method of Wind for determining water retention and hydraulic conductivity was applied (Tamari *et al*., 1993) on larger samples (200 cm^3). The soil water retention curves (□(h)) of smaller samples (100 cm^3) were determined through use of the tension table (Dane and Hopmans, 2002). The water retention and hydraulic conductivity experimental data were parameterised according to the Mualem-van Genuchten relationship (van Genuchten, 1980). Constitutive hydraulic functions where applied in a 2D simulation model (Hydrus 2D, Simunek *et al*., 1999). This model enable us to simulate the soil water balance of slope assuming a defined length and soil depth, and an infinite width. Runs were performed on the same soil simulating the water balance in presence and absence of roads or cliffs. This was obtained changing the boundary conditions: (i) free drainage in case of pedo-continuity and (ii) a seepage face in case of pedo-discontinuity due to roads or cliffs. Runs were also performed to compare soil water balance on two soils on North and South slope (Basile *et al*., 2003).

Results

The main features of the investigated sites where the catastrophic landslides occurred are given in Table 1. Almost all the sites refer to very steep mountain environments having different aspects and geologies. All sites have a forest land use, generally chestnut. The landslides have generally occurred in a very large number and with different rainfall intensity. The number of victims and damages are typically related to the presence of urban settings along the flows rather than to the landslide magnitude.

Table 1. Main features of landslides and detachment crowns (det. = detachment; (l) = data obtained from literature).

Location	Date (l)	Landslide type (l)	Elevation range of det. crown (m asl)	Slope range of det. crowns	Main aspect	Main land use	Main bedrock	Number of land-slides (l)	Rain peak (l)	Vic-tims (l)
Albaredo (Lombardia)	16/11/02	Soil slip-debris flows	1000-1100	41°-50°	W	Grassland with chestnut	Metamorphic rocks	50	230mm /60h	0
Versilia (Toscana)	19/6/96	Soil slip-debris flows	300-900	31°-45°	NE	Chestnut forest	Metamorphic arenaceous rocks & Phyllitic schist	647	400mm /6h	14
Salerno (Campania)	26/10/54	Soil slip-mud flows	200-800	40°-50°	N	Chestnut forest	Limestone	NA	504mm /24h	> 300
Sarno (Campania)	5/5/98	Soil slip-debris/earth flow	700-950	33°-55°	SW	Chestnut forest	Limestone	100	173mm /48h	159
Platì (Calabria)	16/10/51	Soil slip-debris flows	700-1100	40°-50°	SE	Mixed forest (Chestnut - Oak)	Metamorphic rocks	NA	1495mm /72h	19
Giffone (Calabria)	29/6/05	Soil slip	500-1000	38-45°	NW	Chestnut forest	Granite	NA	NA	NA

The most important morphological and chemical features of these soils are given in table 2. All soils are rather deep, they frequently have some kind of vertical discontinuities (e.g. buried soils) and have a dominant sandy loam texture. The soil structure of surface horizons is always granular with a rather high organic C content. pH ranges from acid to neutral, and most importantly all soils show striking andic features ranging from high (Alo+0,5Feo>2%) to moderate ((Alo+0,5Feo:1-2%). The andic features range from silandic in southern sites to aluandic in Northern sites but some of these andic soils do not fulfil WRB requirements for Andosols. In fig. 1 some water retention curves referring to the most important soil horizons of the investigated sites are reported. The curves show a striking homogeneous behaviour with a very high water retention over all pressure heads but especially near saturation. In fact water content at saturation is comprised between a minimum of 0.52 $cm^3\ cm^{-3}$ till a maximum of 0.78 $cm^3\ cm^{-3}$. Moreover, these are very permeable soils according to their very high saturated hydraulic conductivity (data not shown).

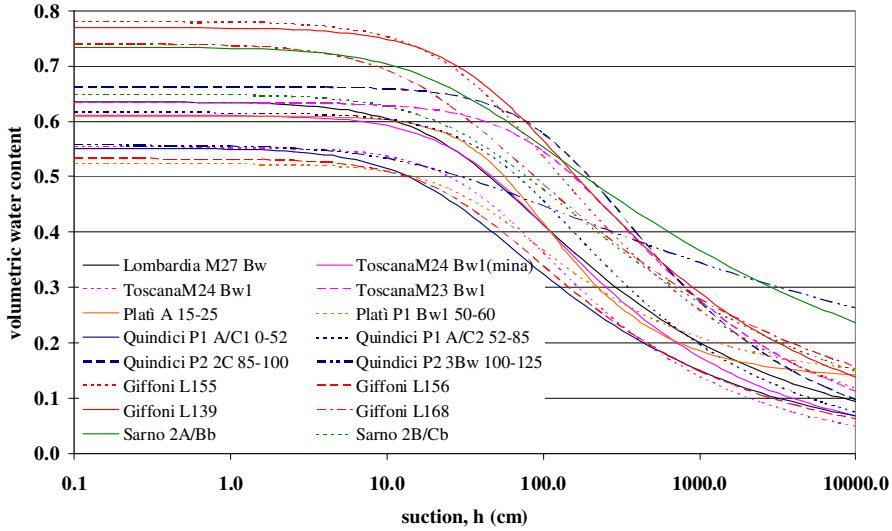

Figure 1. Water retention curves of representative soil horizons of the investigated sites.

At more local scale, discontinuities in the soil cover (i.e. abrupt slope change, road cut) were also modelled and the resulting effects were shown in Fig.2 where the time evolution of soil water storage in the profile (2 m) is reported, both for pedo-continuity (P-C) and pedo-discontinuity (P-DC) simulations. The results refer to the same vertical section located at 100 m from the up slope position. The increase in water storage due to the boundary effects ranges from 30% in the rainy days till 45% in the dryer period. This increases the soil weight and reduces the effective stress inside the soil: therefore, the P-DC condition will increase the risk of instability of the pyroclastic slope cover.

Table 2. Most important features (FAO, 1990) of the soils in the detachment crowns of the investigated landslides.

Abbr.S: sandy; Si: silty; L:loam; G: granular, SB subangular blocky, m: medium, c: coarse,wd :weakly developed; md: moderately developed; sd: strongly developed

Profile	Horizon	Boundaries (cm)	Texture	Structure	Carbonates	pH (H_2O)	Organic C (g kg^{-1})	Alo+0,5Feo (%)	Alp/Alo
Sarno-P1	A	0 - 20	SL	G m, wd	none	7,3	98,5	4,99	0,25
(Campania)	Bw	20 - 38	SL	SB m, wd	none	7,5	10,7	2,46	0,05
	Bc	38 - 71	LS	SB c, wd	none		4,2	5,68	0,00
	C	71 - 100			none	7,5			
	2A/Bwb	100 - 140	SL	SB c, wd	none		10,5	2,05	0,06
Salerno -M25	A	0 - 9	SL	G c, sd	none	7,3	58,0	4,47	0,04
(Campania)	Bw1	9 - 28	SiL	SB m, sd	none	7,4	24,3	4,95	0,03
	Bw2	28 - 48	SiL	SB m, md	none	7,6	15,60	5,47	0,02
	Bw3	48 - 70	SiL	SB m, md	none	7,8	9,60	3,49	0,05
Versilia M24	OA	0-2	S	G c, sd	none	4,1	178,80	0,24	1,00
(Toscana)	Bw1	2-65	SL	SB c, md	none	4,8	12,92	0,50	1,00
	Bw2	65-150	SL	SB m, md	none	4,6	9,55	1,03	0,64
Albaredo-	A	0-40	S	SB m, md	none	5,1	32,00	1,35	0,73
M27_3	Bw	40-110	SL	SB m, md	none	5,3	11,03	1,82	0,19
(Lombardia)									
Platì	A	0-45	L	G c, md	none	5,1		1,35	1,08
(Calabria)	Bw1	45-90	CL	SB m, md	none	5,1	24,97	1,53	0,48
	Bw2	90-120			none	5,2	18,90	1,26	0,54
	BC	> 120				6,0	19,80	0,85	0,39
Giffone	A1	0-15	SL	G m, sd	none	5,1	51,40	1,53	<0,5
(Calabria)	A2	15-30	SL	SB m, md	none	5,0	49,41	2,26	<0,5
	Bw1	30-50	SL	SB m, md	none	5,3	30,95	2,37	<0,5
	Bw2	50-80	SL	SB m, md	none	5,6	25,65	1,60	
	2Ab	80-110	SL	SB m, md	none	5,5	30,11	2,24	
	3Bw1	110-150	SL	SB c, md	none	5,6	16,98	1,83	
	3Bw2	150-200	SL	SB c, md	none	6,0	1,76	0,72	

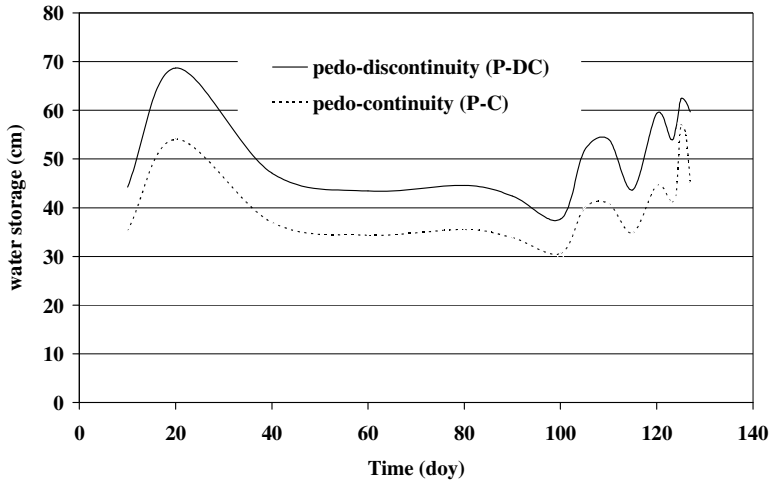

Figure 2. Effects of pedo-continuity (undisturbed slope) and pedo-discontinuity (seepage face) on soil water storage.

Conclusions

The study of soils in the detachment crown of the investigated catastrophic landslides in Italy clearly shows that despite the large differences in geological and climatic settings soils are rather similar and show similar morphology and both andic features and high water retention features. Overall the results at the Italian scale seem to reveal an evident cause-effect between andic soils and the investigated catastrophic mudflows/debrisflow. This is important considering that non-andic non-sliding soils are very much reported in the available soil maps of the investigated landscapes. We believe that andic soils, because of the unique physical properties (hydrological properties, high susceptibility to liquefaction, etc.) induce high landslide vulnerability. We also believe that hydropedology should be added to classical approaches to ameliorate the understanding and the risk assessment of these complex phenomena.

These findings are of primary importance and prove the need of using soil information for classifying zones of different landslide hazard risk (landslide hazard assessment). We also believe that our findings are important also in stimulating similar studies in other areas of the world, especially but not exclusively volcanic, where this type of landslides occur.

References

Bascomb CL (1968) Distribution of pyrophosphate-extractable iron and organic carbon in soils of various groups. *Journal of Soil Science* **19**, 251-268

Basile A, Mele G, Terribile F (2003) Soil hydraulic behaviour of a selected benchmark soil involved in the landslide of Sarno 1998. *Geoderma* **117**, 331-346.

Dane JH, Hopmans JW (2002) Soil Water Retention and Storage - Introduction. In 'Methods of 555 Soil Analysis. Part 4. Physical Methods' (Eds. Dane JH, Topp GC), pp. 671-674. Soil Science Society of 556 America Book Series No. 5.

FAO (1990) Guidelines for Soil Description. 97 pp. FAO, Rome, Italy.

Hungr O, Evans SG, Bovis MJ, Hutchinson JN (2001) A Review of the Clas-sification of Landslides of the Flow Type. *Environmental & Engineering Geoscience* **7**, 221-238.

Klute A, Dirksen C (1986) Hydraulic conductivity and diffusivity: Laboratory methods. In 'Methods of soil analysis, Part 1, Physical and Mineralogical Methods' pp. 687-734. 2nd ed. Agronomy 9 (2). American Society of Agronomy. Madison, Wisconsin.

Parfitt RL (1990). Allophane in New Zealand - a review. *Aust, J, Soil Res.* **28**, 343-360.

Simunek J, Sejna M, van Genuchten MTh (1999) The HYDRUS-2D Software Package for Simulating the Two-Dimensional Movement of Water, Heat, and Multiple Solute in Variably-Saturated Media. Ver. 2.0. U.S. Salinity Laboratory, ARS, USDA, Riverside, CA, USA, pp 228.

Schwertmann U (1964) Differenzierung der Eisenoxide des Bodens durch Extraktion mit Ammoniumoxalat-Lo¨ sung. *Zeitschrift Pflanzenerna ¨hr. Dungung Bodenkunde* **105**, 194-202.

Tamari S, Brukler L, Halbertsman J, Chadoeuf J (1993). A simple method for determining soil hydraulic properties in the laboratory. *Soil Science Society American Journal* **57**, 642-651.

van Genuchten, M. Th., 1980. A closed-form equation for predicting the hydraulic conductivity of unsaturated soils. *Soil Sci. Soc. Am. J.* **44**, 892-898.

Impact of drainage on soil evolution: A morphological quantitative approach

S. Cornu[A, C], D. Montagne[B], J. Darousin[C], I. Cousin[C]

[A]INRA, UR 1119 Géochimie des Sols et des Eaux, Europôle de l'Arbois, BP80, 13545 Aix en Provence Cedex 4, France
[B]UMR INRA/AgroParisTech Environment and Arable Crops, Avenue Lucien Brétignières, 78850 THIVERVAL-GRIGNON, France
[C]INRA, UR 0272 Science du sol, Centre de recherche d'Orléans, 2163 Avenue de la Pomme de Pin, CS 40001 ARDON, 45075 Orléans Cedex 2, France

Abstract
In order to better understand the process of morphological degradation and the impact of drainage on this process, morphological evolution of soil volumes was studied using image analysis of decimetric soil monoliths in Albeluvisol sampled along a soil sequence perpendicular to a drain. The geomorphological interrelationships of four different volume types (black, white-grey, pale-brown and ochre) are quantified. Results show that morphological degradation progresses by the progressive transformation of the ochre volume into pale-brown from their inner, around porosity, and their border. Black volume is simultaneously formed by centrifugal condensation of Mn into the ochre volume. As the process goes on, with decreasing distance to the drain, the ochre volume is atomised and the black volume is released into the pale-brown matrix. This pale brown matrix is further transformed into a white-grey volume formed into its core by centripetal evolution.

Key Words
Luvisols, agricultural practices, pedogenesis, image analysis

Introduction

Human activities were early recognized as a factor affecting soil evolution (Bidwell and Hole, 1965; Yaalon and Yaron, 1966), but their impact on soil evolution were poorly quantified. Montagne *et al*. (2007, 2008) showed that drainage modifies morphological degradation in Albeluvisols. This phenomenon consists in a combination of eluviation of clay minerals and redox processes (Jamagne, 1978; Pedro *et al*., 1978; Dreissen *et al*., 2001). Over time these elementary soil processes induce the formation of a complex juxtaposition of bleached eluvial soil volume (E) with a residual soil volume of the illuvial Bt-horizon. However the mode of propagation of these processes in soil and their consequences on the geometry of the different soil volumes were, to our knowledges, never studied, neither under natural conditions nor under the influence of soil drainage.
Redox processes evolve through transforming fronts as defined by Boulet *et al*. (1982), Fritsch *et al*. (1986) and Lucas *et al*. (1988) among others. These fronts correspond to a succession of mineralogical and chemical transformations (Fristch *et al.*, 1986). Description of the progression of these fronts as well as the locus of segregation allows characterising soil processes. Such fronts were used to map soil spatial distribution at the landscape scale (Boulet *et al*., 1982; Fritsch *et al*., 1986; Lucas *et al*., 1988) but rarely characterised at a decimetric scale (Lucas, 1989), which is the scale of propagation of the morphological degradation.
In this paper we aimed at demonstrating how the process of morphological degradation propagates with the distance to the drain. We used a meso-morphological approach based on image analysis of pictures of decimetre size from soil monoliths sampled at four distances to the drain. The objective is to identify how the different pedological volumes derived from each other and if the process is centripetal or centrifugal.

Methods

Site and soil

The studied Albeluvisol, developed in Quaternary loam, lies on the crest of the Yonne plateau (France). It is cultivated since at least 200 years and shows the following succession of horizons: (i) the ploughed horizon; (ii) a silty E-horizon; (iii) a horizon constituted by a complex mixture of several soil volumes of distinct colours and called E&Bt-horizon hereafter. Its most abundant volumes are silty and white-grey to pale-brown and its less abundant ones are clayey and ochre with black concretions and impregnations; (iv) the Bt-horizon which upper part is degraded.

In the studied plot, a subsurface drainage network was installed, in 1988 (16 years before sampling), by subsoiling, perpendicular to the main slope, at 1 m depth and spaced 15 m apart. We dug a 4 m long trench perpendicularly to one of the drains, providing the following macroscopic observations. (i) The thickness of the different horizons does not vary along the trench. (ii) As the distance to the drain decreases from 2 to 0.5 m, the

quantity of white-grey, pale-brown and black soil volumes increases both in the E&Bt- and in the degraded Bt-horizons. On the contrary, the clayey ochre soil volume decreases. (iv) Beyond 2 m from the drain, the amounts of the different soil volumes do not change significantly.

Sampling, image acquisition and analysis

We sampled four decimetric soil monoliths in the Eg&Bt- horizon along a soil sequence comprising portions affected and unaffected by soil drainage, at four distances to a drain: 60, 110, 210, and 400 cm, the last distance being considered as a reference. The surface of each monolith (in a horizontal x, y-plane) was photographed in colour (RGB mode) using natural light, with a resolution of 450 µm per pixel. A 1.5 cm slice from the monolith surface was then cut off with a knife. The new face was then photographed. This was repeated over the whole monolith thickness, i.e. 8 times.
Image analysis was based on (i) a supervised training method using ERDAS IMAGINE® (www.erdas.com) to assign the different pixels to the different types of soil volumes and (ii) ArcInfo™ (www.esri.com) for characterisation of the morphology of the different soil volumes.

Results

Morphology of the different soil volumes at the reference position (400 cm to the drain)

At 400 cm to the drain, the surface of the ochre and pale-brown volumes are almost equivalent, each one covering about 45 % of the total surface while the white-grey and black volumes exhibit considerably smaller surfaces (less than 10 % each) (Figure 1). The ochre volume mainly neighbours the pale-brown one, the black volume the ochre one, and the white-grey volume the pale-brown one. The lengths of the perimeter of the different pedological volumes rank like their relative surfaces; however, the ratio perimeter/surface (called relative perimeter for simplicity) of the different volumes is larger for the black volume, followed by the white-grey volume. The smallest relative perimeters are recorded for the ochre and pale-brown volumes.
A pedological volume is composed of several distinct items for which some characteristics (number, surface, etc.) were quantified. At 400 cm to the drain, the different pedological volumes are in about the same number of items. But if the number of items composing a pedological volume is considered relative to its surface, the larger numbers of items are recorded for the black volume, followed by the white-grey volume. These numbers are much smaller for the ochre and pale-brown volumes than for others.
Some pedological items include items of another pedological volume: the last can be considered as a hole in the first (Figure 1). These holes are mainly located in the ochre and pale-brown volumes. They are mainly black and pale-brown in the ochre volume and mainly white-grey and ochre in the pale-brown volume (Figure 1).
From these results we can conclude that pale-brown and ochre volumes consist in large items and that white-grey and black soil volumes occur as small items embedded into respectively the pale-brown and ochre volumes. The morphological relationship between pale-brown and ochre volumes is more complex as both form holes in the other. As the ochre volume is considered as residuals, this morphological distribution means that ochre volume is transformed into pale-brown volume both from its core and its border, white-grey volume being a further evolution step occurring only in the pale-brown volume.

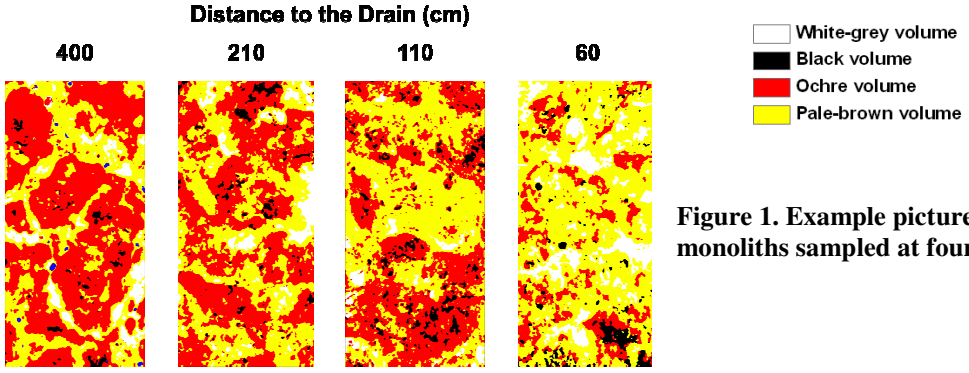

Figure 1. Example pictures representative of the monoliths sampled at four distances to the drain.

Evolution of the volume morphology with the distance to the drain

The relative surface of the different pedological volumes varies with the distance to the drain: the ochre volume surface decreases significantly with the distance to the drain, while the surface of the other volumes increases (Figure 2).

The contact length between the ochre and the pale-brown and between the black and the ochre volumes increases significantly when moving from 400 to 210 and 110 cm to the drain respectively and then decreases significantly from 110 to 60 cm to the drain, while the length of contact between white-grey and pale-brown volumes is significantly higher at 60 cm to the drain. At this last position, the black volume comes into contact with the pale-brown one.
While the distance to the drain decreases, the perimeter of the white-grey, black and pale-brown volumes increases significantly (Figure 2). The perimeter of the ochre volume increases significantly from 400 to 210 cm to the drain, stabilizes from 210 to 110 cm and then decreases significantly from 110 to 60 cm. In terms of relative perimeter, the only significant variations observed with the decrease of the distance to the drain are an increase for the ochre volume and a decrease for the pale-brown one.
While the distance to the drain decreases, the total number of items increases significantly for three of the four soil volumes (black, white-grey and ochre; Figure 2). The number of items of the pale-brown volume increases significantly from 400 to 210, stabilizes from 210 to 110 cm and then decreases significantly from 110 cm to 60 cm to the drain.
The relative number of items of the ochre volume increases significantly as the distance to the drain decreases. The relative number of items for the black volume increases significantly from 400 to 210 cm and decreases to return to its initial value for distances below 2 m to the drain. No trend with the distance to the drain is observed for the relative number of items of the white-grey volume, while this relative number is significantly lower at 60 cm to the drain than at the other distances for the pale-brown volume.
The number of holes in the ochre volume significantly increases from 400 to 110 cm to the drain and then sharply decreases at 60 cm just as the number of holes in the pale-brown volume increases suddenly (Figure 2). These trends are also observed as the number of holes per surface unit is considered. The number of black holes in the ochre volume increases from 400 to 100 cm to the drain and then decreases strongly to reach, at 60 cm, the number observed at 400 cm. The number of pale-brown holes increases when moving from 400 to 210 cm, stabilizes from 210 to 110 cm and decreases, when moving to 60 cm, to half that number at 400 cm. In terms of surface of the holes, the evolution with the distance to the drain is somewhat different. The surface of the black holes in the ochre volume is stable from 400 to 210 cm to the drain, but increases from 210 to 110 cm and then decreases strongly at 60 cm with a surface at 60 cm half of that measured at 400 cm. The surface of the pale-brown holes increases slightly from 400 to 210 cm to the drain and then decreases until 60 cm.
The number of ochre holes in the pale-brown volume increases from 400 to 210 cm then stabilizes, while the number of white-grey holes increases at 60 cm. The surface of the ochre holes increases from 400 to 60 cm to the drain, while the situation is more complex for the white-grey holes with nevertheless a higher surface at 60 cm.

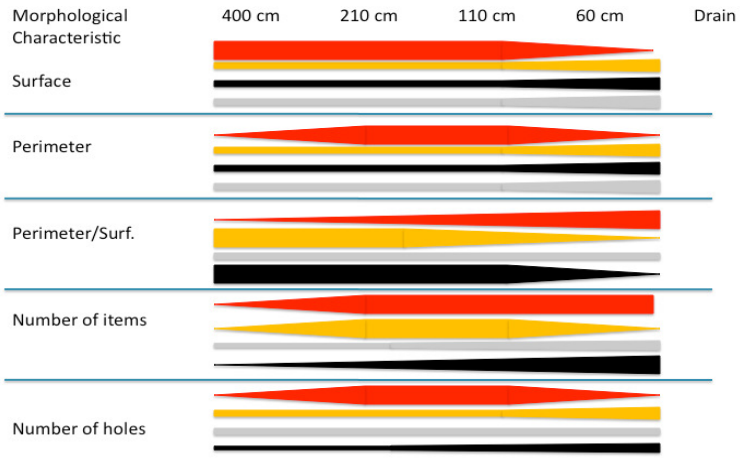

Figure 2. Evolution with the distance to the drain of the main morphological characteristics for the different soil volumes: ochre (in red), pale-brown (in yellow), black (in black) and white-grey (in grey).

We calculated the constant of Euler-Poincaré for the different soil volumes at the different distances to the drain. This constant represents the connectivity of a volume: it is positive for disconnected objects and negative for objects with redundant connections, i.e. with holes. In the studied images, the constant is positive for the white-grey and black volumes and negative for the pale-brown volume whatever the distance to the drain. For the ochre volume, the constant is negative from 400 to 110 cm to the drain and positive at 60 cm to the drain, meaning that, at this last distance, the ochre volume is composed by small disconnected items, while it was

constituting a more or less connected matrix with the pale-brown volume at the other distances (Figure 1). These results show that, with the distance to the drain, the ochre volume that constitutes the matrix at 400 cm to the drain is progressively transformed into a pale-brown volume. The black volume is first formed into the ochre volume and then released into the pale brown matrix at 60 cm to the drain where the ochre volume partially disappears. Transformation of the ochre volume into pale-brown occurs both by the inner of the ochre items, around pores, and at the border of the ochre items. The process acts first by indentation of the ochre items, from 400 to 110 cm to the drain, that are then atomised at 60 cm to the drain.

Conclusion

Montagne *et al*. (2008) showed that the black volume has the same composition in clay and goethite than the ochre one, but are slightly richer in ferrihydrate and largely in Mn-oxides, while the pale-brown volume is mainly impoverished in goethite and ferrihydrite and the white-grey volume is further impoverished in those minerals and in Mn-oxides compared to the ochre volume. The morphological analysis confirms that the pale-brown volume results from the alteration of the ochre volume and the white-grey one from the further alteration of the pale-brown volume as no white-grey volume was recorded in contact with the ochre one. This analysis also confirms that black volume results from the centrifugal condensation, into the ochre volume, of Mn and secondarily Fe released from the alteration of the ochre volume. As the process progresses along the drainage sequence, progressive indentation and final atomisation of the ochre volume is responsible for the release of the black volume into the pale-brown matrix. Ochre volume alteration takes place both at the border and in the volume, along pores, as demonstrated by the geometry of the pale-brown and ochre volumes. Finally, the formation of the white-grey volume from the pale-brown one occurs in the core of this last one and is centripetal.

These preliminary results allow concluding that the transformation evolutions by drainage are both centrifugal and centripetal. Centrifugal evolutions of the ochre volumes can be due to physical transfer of particles via preferential flows occurring in the clear volumes, while centripetal evolution could correspond to the redox processes. Quantification of the respective importance of centrifugal versus centripetal evolution will thus allow quantifying the relative importance of the two processes in the morphological degradation phenomenon that is well spread in soils but still insufficiently characterized.

References

Bidwell OW, Hole FD (1965) Man as a factor of soil formation. *Soil Science* **99**, 65-72.

Boulet R, Humbel FX, Lucas Y (1982) Analyse structurale et cartographie en pédologie. II - Une méthode d'analyse prenant en compte l'organisation tridimentionnelle des couvertures pédologiques. Cah. *ORSTOM, série Pédologie* **XIX(4)**, 323-339.

Driessen P, Deckers J, Spaargaren O, Nachtergaele F (Editors) (2001) Lecture Notes on the Major Soils of the World. FAO, Rome, 334 pp.

Fritsch E, Bocquier G, Boulet R, Dosso M, Humbel FX (1986) Les systèmes transformants d'une couverture ferrallitique de Guyane française. *Analyse structurale d'une formation supergène et mode de représentation. Cah. ORSTOM, série Pédologie* **XXII(4)**, 361-395.

Jamagne M (1978) Soil-forming processes in a progressive evolutionary sequence on loessial silty formation in a cold and humid temperate zone. *Comptes Rendus Hebdomadaires des Séances de l'Académie des Sciences, Paris* **286(1)**, 25-27.

Lucas Y, Boulet R, Chauvel A (1998) Intervention simultanée des phénomènes d'enfoncement vertical et de transformation latéral dans la mise en place de systèmes de sols de la zone tropicale humide. *Cas des systèmes sols ferrallitiques-podzols de l'Amazonie Brésilienne. C.R.A.S., série II.* **306**, 1395-1400.

Lucas Y (1989) Systèmes pédologiques en Amazonie brésilienne. Equilibres, déséquilibres et transformations. PhD, University of Poitiers.

Montagne D, Yahiaoui M, Cousin I, Le Forestier L, Cornu S (2007) Quantification of soil volumes in the Eg & Bt-horizon of an Albeluvisol using image analysis. *Can. J. Soil Sci.* **87**, 51-59.

Montagne D, Cornu S, Josière O, Le Forestier L, Daroussin J, Cousin I (2008) Soil drainage as a factor of human-induced soil evolution: quantification of such an evolution in an Albeluvisol. *Geoderma* **145(3-4)**, 426-438.

Pedro G, Jamagne M, Begon JC (1978) Two routes in genesis of strongly differentiated acid soils under humid, cool-temperate conditions. *Geoderma* **20**, 173-189.

Yaalon DH and Yaron B (1966) Framework for man-made soil changes: an outline of metapedogenesis. *Soil Science* **102(4)**, 272-277.

Ischia landslides (Italy): A multidisciplinary approach aimed to increase knowledge of soil properties

Simona Vingiani[A], Roberto De Mascellis[B], Giacomo Mele[B], Nadia Orefice[B], Luciana Minieri[A], Fabio Terribile[A]

[A] Faculty of Agricultural Science, Department of Soil, Plant, Environmental and Animal Production Science, University Federico II of Naples, Portici (NA) Italy, Email vingiani@unina.it
[B] CNR-ISAFOM Institute for Agricultural and Forest Systems in the Mediterranean, Ercolano (NA) - Italy, Email roberto.demascellis@cnr.it

Abstract
An integrated approach (chemical, hydrological, mineralogical and micro-tomographic) has been used to study the soils of the landslides occurred in the Ischia island (Italy) on April 2006. The study has been carried out on three soil profiles sampled on representative detachment crowns. The main outcome indicates: (i) presence of volcanic soils, very rich in primary glass, characterised by the presence of poorly ordered kaolinite in all horizons and expandable clay minerals only in the deepest horizons (CBb and Cb), (ii) high values of water content near saturation for all soil horizons, (iii) a relevant vertical discontinuity of soil physical properties. In particular, the deep silty horizon (Cb) retains high amounts of water at low matric potential and shows the lowest value of saturated hydraulic conductivity than the other horizons. This micro-tomographic analysis of this deep horizon indicates a very complex intra-aggregate pore space, which seems an important factor influencing the specific rheological behaviour of this sliding horizon.
In terms of pedogenetic processes, the soils of M. Vezzi northern slope are very different from those described for other catastrophic landslides of the Campania region (Sarno, Quindici, etc.), but they have in common the presence, along the soil profile, of marked physical discontinuities surely contributing to the initiation mechanisms of the landslides.

Key Words
Volcanic soils, hydrological properties, micro-tomography, soil mineralogy, Campania landslides

Introduction

In this paper are presented the preliminary results of a pedological study regarding landslides that occurred on April 30th 2006, on the top of the northern slope of Monte Vezzi, in the Ischia island (South Italy). The type of mechanism occurred during these landslide events is classified as a complex debris slide - debris flow, with an intermediate phase of debris avalanche *(*De Vita *et al.,* 2007). It appeared very similar to phenomena affecting slopes of the Campania calcareous reliefs over many years. In fact, the Campania region has a long history of landslide events. Recent data (years between 1580 and 2002) indicate 453 landslides producing damage to people, leading more than 1300 deaths (SICI, 2007). In spite of the social relevance of these events and, in many cases, the large evidence of the crucial role of the pedological control in these phenomena, soil studies in landslide areas are not so common in Italy, in particular in the Campania region. Since 1999, chemical and physical properties were measured on the soils of the detachment crowns of Sarno and Quindici (Terribile *et al.,* 2000) and 19 other Campania landslides, chosen as catastrophic in terms of human life and damages to infrastructures and occurred in the last century in this region (Terribile *et al.,* 2007). Results showed an important relationship between landslides and Andosol occurrence. Andosol's (WRB, 2006) susceptibility to landslides is known and has been related to some of their physical properties, being the control factors that induce remarkable fragility to ecosystems: i) low adhesion to substrates (Yamanaka, 1964), ii) materials with low inner cohesion (Maeda *et al.,* 1977), iii) high water retention and high saturated hydraulic conductivity (Maeda *et al.,* 1977; Basile *et al.,* 2003). Nevertheless, the volcanic soils of Ischia landslides are younger and seem less weathered than those found on the carbonatic reliefs of the Campania region and, according to a preliminary study (Vingiani and Terribile, 2007), they do not exhibit andic properties, suggesting that not only Andosols slide down in these areas. An integrated approach (chemical, hydrological, mineralogical and micro-tomographic) has been considered to be fundamental in order to better investigate the complexity of these unique volcanic covers in relation to landslide events.

Methods

Three representative soil profiles (according to slope gradient, undisturbed soils, etc.), approximately 250 cm deep, one for each landslide detachment crown, have been described and sampled. Air dried and sieved (less

than 2 mm) soil samples have been analysed chemically, according to the Official Methods of Soil Analysis (Page *et al*., 1982). Due to the volcanic context, specific chemical analysis for Andosol classification have been carried out: phosphate retention (Blackemore *et al.,* 1987), ammonium oxalate (Schwertmann, 1964) and Na-pyrophosphate (Bascomb, 1968) selective extractions. Particle size measurements were performed by means of laser diffraction technique (LD) using a Malvern Mastersizer 2000 system®, after soil dispersion by Na-hexametaphosphate. This dispersant agent is efficient in the case of absence or scarce andic properties. Mineralogical analysis, by means of X-ray diffractometry (XRD), has been carried out on sand, silt and calcium saturated clay fractions and patterns have been acquired by a Rigaku Geigerflex D/Max IIIC®, with Ni filtered CuKa radiation at 35 kW and 35 mA. Undisturbed soil samples approximately 400 cm^3 in volume were collected in each pedological horizon to determine the hydrological properties. The saturated hydraulic conductivity, *Ks,* was measured by means of a constant head permeameter (Klute and Dirksen, 1986). Both $\theta(h)$ relationship, between water content θ and water pressure head *h,* and $K(\theta)$ relationship, between hydraulic conductivity *K* and water content, were determined applying the evaporation method (Wind, 1968; Tamari *et al*., 1993). During a 1-dimensional transient upward flow due to the evaporation process, an automated system acquired weights of the soil samples and pressure head data from pressure transducers connected to three tensiometers for each sample. To determine the points of the $\theta(h)$ curve for higher values of *h* a pressure apparatus was used. X-ray micro-tomographic scanning has been performed on 30 mm^3 of soil aggregates, obtained by sieving the bulk soil at 2 mm, using the SKYSCAN 1172 desktop system (www.skyscan.be) based on a microfocus cone beam source. The intra-aggregate three-dimensional pore structure has been reconstructed at 3 microns pixel resolution using an optimised inverse Radon transform (Kak and Slaney, 1988). Intra-aggregate pores have been visualized using Image ProPlus software (www.mediacy.com) and analyzed using the "opening" algorithm to calculate the pore size distribution (Serra 1982) and the procedure of Lantuejoul and Maisonneuve (1984) to calculate the percolation curves in order to evaluate the connectivity of the pore space.

Results

All soils are characterised by thin (5 cm) very dark brown (10YR 2/2) organ-mineral topsoils, with abundant (40%) small (2-5 mm) coarse fragments. The subsoil, from dark yellowish to olive brown (10YR 4/4 - 2.5Y 4/3), is increasingly moist with depth, and skeletic (more than 50% of coarse fragments), till the depth of 170 cm, where greyish brown (2.5Y 5/2), not massive, ashy horizons, with few (less than 4%) coarse fragments, occurs (CBb and Cb horizons). As follow, only results of the more representative soil profile (P2) are presented and discussed. Some chemical and physical properties of the P2 soil profile are reported in table 1.

Table 1. Some chemical and physical properties of the P2 profile.

Horizon	Depth (cm)	OC	pH		PR	Alo +0.5 Feo	*Ks*
		g kg^{-1}	H_2O	KCl	%	%	cm h^{-1}
A	0-5	71.3	6.7	6	31.6	0.47	n.d.
Bw1	5-50	5.9	7.1	5.7	22.1	0.43	102.9
Bw2	50-90/110	5.5	7.3	5.7	21.4	0.45	144.7
ABb	110-130/140	4.7	7.1	5.1	17.2	0.26	n.d.
Bb	140-170	2.7	7.3	5.4	14.6	0.21	24.5
CBb	170-215	1.3	7.2	5.0	7.8	0.10	31.9
Cb	215-220+	1.2	7.3	4.8	3.5	0.07	5.7

PR= phosphate retention; Ks= saturated hydraulic conductivity; n.d. = not determined

The results of the particle size distribution analysis evidenced a main bimodal distribution of soil particles, from the top of the profile to 170 cm, while a general unimodal distribution below 170 cm (CBb and Cb horizons), confirm the presence of a marked textural discontinuity at that depth, not only in terms of coarse fragments (Figures 1a and 1b).

Mineralogical analysis indicates the presence of K and Na feldspars and mica, in both sand and silt fractions, while analcime has been detected mainly in the silt fraction. The clay fraction analysis evidenced presence of kaolinite in all the soil horizons, while expandable clay minerals have been found only in the C horizons (CBb and Cb). Some of the measured water retention curves are plotted in figure 2. They show high values of water content near saturation (more than 0.6 cm^3/cm^3) and also along the whole range of pressure heads.

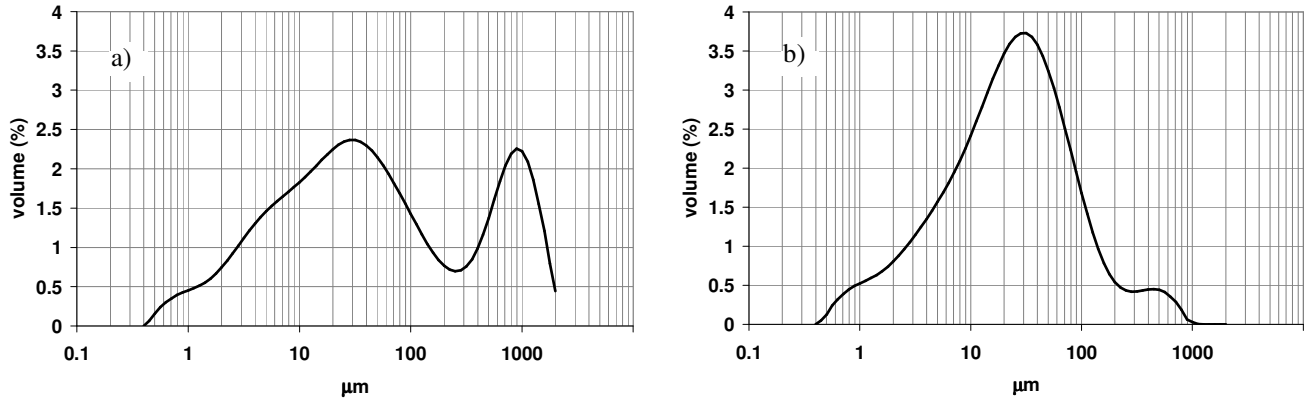

Figure 1. Particle size distribution of the ABb (a) and Cb (b) horizons.

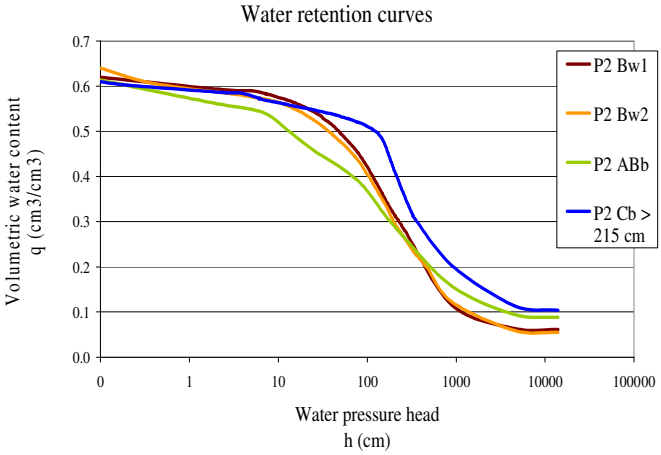

Figure 2. Water retention curves of some P2 soil horizons.

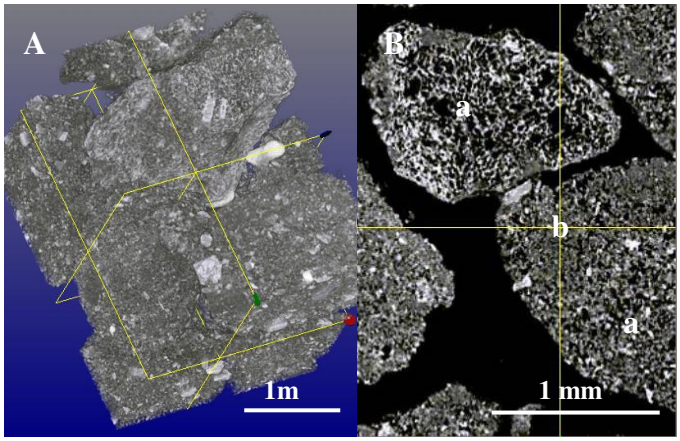

Figure 3. µCT-generated (A) three and (B) two-dimensional images of soil aggregates from the Cb horizon.

In particular, the Cb horizon, compared to the more structured upper horizons, shows high values of water retention for high values of tension and a drastic change of the slope of the retention curve for a tension value of about 130 cm. In table 2 are shown some of the *Ks* values determined by laboratory measurements. The values are high, in agreement with the well drained soil profile characteristics, but there is an important decrease of the saturated hydraulic conductivity in the deepest horizon Cb.
The three-dimensional visualisation of the Cb horizon intra-aggregate space (Figure 3) shows two different arrangements: the first (Figure 3B-b) is relative to large pumice grains and the second (Figure 3B-a) to smaller particles (generally of the silt size) constituting the soil matrix. The quantification of the intra-aggregate pore architectures by 3D image analysis (data not given in this paper) confirms the presence of larger pores (30 µm estimated mean diameter) in the pumice structure, as compared to the soil matrix consisting of smaller particle (10 µm estimated mean diameter) arrangements. Both pore systems showed an overall isotropic fully connected porosity. Results of the micro-tomographic analysis (not yet completed) seem coherent with data on the hydraulic properties.

Conclusions

This work led to a first knowledge about the soil properties of the M. Vezzi northern slope, in the Ischia island, through the use of a multidisciplinary (chemical, mineralogical, hydrological and micro-tomographic) approach. Results evidenced, along the soil profile, the presence of a marked discontinuity in terms of clay mineralogy, particle size distribution and hydraulic properties corresponding to a deep horizon (170 cm), whose upper limit is considered the sliding surface of the soil materials involved in the landslides. First data on the complex intra-aggregate pore space of this deep horizon showed the presence of a fully connected porosity, whose ongoing analysis is expected to give a contribution to the knowledge of the causes of water drainage reduction in the soil profiles, considered to be a primary cause of landslides.

References

Basile A, Mele G, Terribile F (2003) Soil hydraulic behaviour of a selected benchmark soil involved in the landslide of Sarno 1998. *Geoderma* **117**(3, 4), 331-346.

Bascomb CL (1968) Distribution of pyrophosphate extractable iron and organic carbons in soils of various groups. *J. Soil Sci.* **19**, 251-268.

Blakemore LC, Searle PL, Daly BK (1987) Methods for Chemical Analysis of Soils. N.Z. Soil Bureau Sci. Rep. 80. Soil Bureau, Lower Hutt. New Zealand.

De Vita P, Di Clemente E, Rolandi M, Celico P (2007) Engineering geological models of the initial landslides occurred on april 30 2006, at the Mount of Vezzi (Ischia island, Italy). Italian Journal of Engineering Geology and Environment. University of Rome La Sapienza, Research Center CERI, n2.

Kak AC, Slaney M (1988) Principles of Computerized Tomographic Imaging,. IEEE Press.

Klute A, Dirksen C (1986) Hydraulic conductivity and diffusivity: Laboratory methods. In 'Methods of Soil Analysis, Part 1, Physical and Mineralogical methods. 2nd ed. Agronomy 9 (2), pp. 687-734. (American Society of Agronomy, Madison, Wisconsin).

Lantuejoul C, Maisonneuve F (1984) Geodesic methods in quantitative image analysis. *Pattern Recognit.* **17**, 177-187.

Maeda T, Takenaka H, Warkentin BP (1977) Physical properties of allophane soils. *Adv. Agron.* **29**, 229-264.

Page AL, Miller RH, Keeney DR (1982) Methods of Soil Analysis. Part 2 – Chemical and Microbiological Properties. Second Edition. SSSA.

Schwertmann U (1964) Differenzierung der Eisenoxide des Bodens durch photochemische Extraktion mit saurer Ammoniumoxalat-losung. *Zeitschrift Pflanzenernahrung Dungung Bodenkunde* **105**, 194-202.

Serra J (1982) Image analysis and mathematical morphology. Academic Press, London.

SICI - Sistema Informativo Catastrofi Idrogeologiche (2007). Dati storici. Danni alle persone in Campania.http://wwwdb.gndci.cnr.it/php2/danni/danni_regione_a.php?lingua=it

Tamari S, Bruckler L, Halbertsma J, Chadoeuf J (1993) A simple method for determining soil hydraulic properties in the laboratory. *Soil Sci. Soc. Am. J.* **57**, 642-651.

Terribile F, Basile A, De Mascellis R, Di Gennaro A, Mele G, Vingiani S (2000) I suoli delle aree di crisi di Quindici e Sarno: proprietà e comportamenti in relazione ai fenomeni franosi. *Quaderni di Geologia Applicata* **7**(1), 59-79.

Terribile F, Basile A, De Mascellis R, Iamarino M, Magliulo P, Pepe S, Vingiani S (2007) Landslide processes and Andosols: the case study of the Campania region, Italy. In 'Soils of Volcanic Regions in Europe: Volcanic Soils and Land Use', pp. 545-563. (Eds. Arnalds, Bartoli, Buurman, Oskarsson, Stoops, Garcìa-Rodeja) Springer.

Vingiani S, Terribile F (2007) Soils of the detachment crowns of Ischia landslides. Italian Journal of Engineering Geology and Environment. University of Rome La Sapienza, Research Center CERI, n2, 51-63

Wind GP (1968) Capillary conductivity data estimated by a simple method. In 'Water in the unsaturated zone Int. Assoc. Sci. Hydrol. Vol. 1', pp. 181-191. (Eds. Rijtema PE, Wassink H). (UNESCO, Paris).

WRB (World Reference Based For Soil Resources) (2006) A framework for international classification, correlation and communication. Food and Agriculture Organization of the United Nations (FAO).

Yamanaka K (1964) Adhesion. In "Volcanic Ash Soils in Japan Chapter 4, Physical. Properties", pp. 69-75. (Eds. Yamanaka K, Black CA).

Nutrient uptake responses of tropical turfgrass species to salinity stress

Md. Kamal Uddin[A*], Abdul Shukor Juraimi[A], Mohd. Razi Ismail[A], Radziah Othman[B] and Anuar Abdul Rahim[B]

[A]Department of Crop Science, Institute of Tropical Agriculture, Universiti Putra Malaysia, Serdang, Malaysia
[B]Department of Land Management, Universiti Putra Malaysia, 43400 Serdang, Selangor, Malaysia.
*Corresponding author. Email mkuddin07@yahoo.com

Abstract
The need for salinity tolerance of turfgrasses is increasing because of the augmented use of effluent or other low quality water (seawater) for turfgrass irrigation. Irrigation seawater of different salinity levels (0, 24, 48, and 72 dS/m) were applied to turfgrass species grown in a plastic pots filled with a mixture of sand and peat (9:1). Increasing salinity reduced uptake of K, Ca, and Mg but increased Na content in the shoot tissue. The lowest K, Ca, Mg content reduction was found in the species of *Paspalum vaginatum* and *Zoysia japonica* while the maximum was recorded in the species of *Digitaria didactyla* and *Cynodon dactylon* 'tifdwarf'. Other species *Zoysia matrella* and *Cynodon dactylon* 'satiri' were intermediate. The overall, shoot K:Na ratio was the highest in *Paspalum vaginatum* followed by *Zoysia japonica*. The results revealed that K, Ca and Mg ions uptake and their distribution to shoot tissues under salinity stress may be relevant issues for plant nutrition along with salt (Na^+) exclusion for salinity tolerance.

Key Words
Salinity stress, Nutrient uptake, Turfgrass, Seawater

Introduction
Salinity is one of the most important abiotic stresses widely distributed in both irrigated and non-irrigated areas of the world and include imposition of ion toxicities (e.g., Na and Cl), ionic imbalances, osmotic stress and soil permeability problems (Ashraf *et al.,* 2008).Salt tolerance in plants is generally associated with low uptake and accumulation of Na^+, which is mediated through the control of influx and/ or by active efflux from the cytoplasm to the vacuoles and also back to the growth medium (Jacoby, 1999). In addition to inorganic ion contributions to osmotic adjustment, genotypic differences in nutrient elements uptake under salinity have implications for maintaining adequate nutrition and for optimizing nutrient/element related salinity tolerance mechanisms. Uptake of essential ions (both cations and anions) including K^+, Ca^{2+}, Mg^{2+}, NH_4^+, and NO_3^- have been reported to be suppressed in various species by high concentrations of NaCl, especially in saline soils and irrigation waters (Rubinigg *et al.,* 2003). So the study on nutrient uptake in tropical turfgrass under salinity stress may be helpful in breeding salt tolerant cultivars by identifying chemical potential of salinity tolerance and the current study is designed to address the aforesaid issues critically.

Methods
The experiment was conducted with six turfgrass species in the glasshouse of Faculty of Agriculture at Universiti Putra Malaysia under sand culture system. The soil was sandy with pH 5.23, EC 0.3 dS/m, OC 0.69%, sand 97.93 %, silt 1.89% and clay 0%. The diameter of plastic pots was 14 cm with 15 cm depth. The average day temperature and light intensity of glasshouse were 28.5-39.5 ^{0}C and 1500-20400 lux respectively. Four saline water concentrations: 0, 24, 48, 72 dS/m were applied in this study. Untreated checks were irrigated with distilled water. Seawater was diluted 50% and NaCl was added to seawater to obtain the salty water level of 48, 72 dS/m respectively. To avoid osmotic shock, salinity levels were gradually increased by daily increments of 8 dS/m until the final salinity levels were achieved. After the targeted salinity levels were achieved, the irrigation water was applied once daily basis for a period of four weeks. At the end of the experiment shoots and roots were harvested and were washed with deioniozed water and dried at 70 ^{0}C for 72 hrs. All elemental analyses were conducted on acid digested material through micro-Kjeldahl digestion system. The content of Na, K, Ca and Mg ions were measured by Atomic Absorption Spectrophotometer (AAS).The experimental design was a randomized complete block design (RCBD) with five replications. The results were analyzed using (SAS 2006) and treatment means were compared using LSD Test.

Results
Sodium content of turf grasses increased and potassium, calcium, magnesium content, K/Na ratio decreased with increasing salinity levels (Table 1,2,3,4,& 5). At 0 dS/m salinity, Na contents in different turf species ranged between 0.52 to 0.59 mg /g dry weights. However, at 24, 48 and 72 dS/m salinity levels, Na uptake

ranged between 6-10, 22-30 and 23-35folds over the control, respectively (Table 1). At 24 dS/m salinity, least Na accumulations were recorded in species *Paspalum vaginatum* (6-fold), *Zoysia japonica* (6-fold), and *Cynodon dactylon* 'satiri' (6-fold); while maximum accumulations were recorded in species *Digitaria didactyla* (10-fold) and *C. dactylon* 'tifdwarf' (8-fold). At 72 dS/m salinity, least Na accumulations were recorded in species *P. vaginatum* (23-fold) and *Z. japonica* (25-fold); while maximum accumulations were recorded in species *C. dactylon* 'tifdwarf' (34-fold) and *D. didactyla* (30-fold).

Table 1. The effect of different salinity levels on shoot Na content of different turfgrass species (Values in the parentheses indicate percent decrease compared to control).

Species	Sodium content in mg /g, dry weight				LSD (0.05)
	Salinity levels (dS/m)				
	0	24	48	72	
C. dactylon 'satiri'	0.52 d (1)	3.23 c (6)	11.50 b (22)	16.48 a (32)	1.70
C. dactylon 'tifdwarf'	0.57 d (1)	4.42 c (8)	17.30 b (30)	19.43 a (34)	1.92
Digitaria didactyla	0.56 d (1)	5.86 c (10)	13.54 b (24)	16.83 a (30)	1.39
Paspalum vaginatum	0.54 d (1)	3.09 c (6)	8.11 b (15)	12.68 a (23)	0.79
Zoysia japonica	0.59 d (1)	3.77 c (6)	11.21 b (19)	14.82 a (25)	0.94
Zoysia matrella	0.55 c (1)	3.87 b (7)	12.53 a (23)	13.65 a (25)	1.17

Means accompanied by common letters in rows are not significantly different at $P \leq 0.05$ by LSD test.
Potassium content of different turfgrass species ranged from 15.38 to 28.97 mg /g dry weight in control treatment (Table 2). At 24 dS/m least reduction was observed in species *P. vaginatum* (4%), *Z. japonica* (6%) and *Z. matrella* (6%) while maximum reduction were found in species *D. didactyla* (33%) and *C. dactylon* 'tifdwarf' (21%) . At 72 dS/m salinity, the lowest K reduction were recorded in species *P. vaginatum* (26%) *and Z. japonica* (30%) while highest reduction was found in species *D. didactyla* (46%).

Table 2. The effect of different salinity levels on shoot K content of different turfgrass species (Values in the parentheses indicate percent decrease compared to control).

Species	potassium content in mg /g, dry weight				LSD (0.05)
	Salinity levels (dS/m)				
	0	24	48	72	
C. dactylon 'satiri'	16.39 a (100)	14.46 b (88)	10.55 c (64)	9.88 c (60)	1.40
C. dactylon 'tifdwarf'	15.65 a (100)	12.38 b (79)	10.06 c (64)	9.70 c (62)	1.83
Digitaria didactyla	15.87 a (100)	10.64 b (67)	10.33 b (65)	8.56 c (54)	1.22
Paspalum vaginatum	28.97 a (100)	27.78 a (96)	24.38 b (84)	21.56 c (74)	1.33
Zoysia japonica	25.40 a (100)	23.92 a (94)	20.40 b (80)	17.95 c (71)	1.48
Zoysia matrella	18.63 a (100)	17.52 a (94)	13.45 b (72)	13.04 b (70)	2.22

Means accompanied by common letters in rows are not significantly different at $P \leq 0.05$ by LSD test

The highest K/Na ratio was found at control treatment and it ranged from 22.36-54.13 (Table 3). The overall, at all salinity levels the highest K/Na value was recorded in *P. vaginatum* followed by *Z. japonica*, on the other hand the lowest value was found in *C. dactylon* 'tifdwarf' followed by *D. didactyla*. The overall, shoot K:Na ratio was highest in *P. vaginatum* and lowest in *C. dactylon* 'tifdwarf'. The relative salt tolerance between species may be related to the maintenance of higher root growth, or high K:Na ratio in the shoot (Qian *et al.,* 2001).

Table 3.The effect of different salinity levels on K/Na ratio of different turfgrass species.

Species	Potassium/Sodium ratio				LSD (0.05)
	Salinity levels (dS/m)				
	0	24	48	72	
C. dactylon 'satiri'	31.39 a	4.52 b	0.92 c	0.61 c	1.28
C. dactylon 'tifdwarf'	27.40 a	2.89 b	0.58 c	0.50 c	0.86
Digitaria didactyla	28.17 a	1.83 b	0.77 bc	0.51 c	1.29
Paspalum vaginatum	54.13 a	9.26 b	3.02 c	1.70 c	3.72
Zoysia japonica	42.86 a	6.37 b	1.82 c	1.21 c	3.14
Zoysia matrella	33.72 a	4.69 b	1.08 bc	0.86 c	3.68

Means accompanied by common letters in rows are not significantly different at $P \leq 0.05$ by LSD test.
On average all the species, Ca (mg /g) content decreased due to increasing salinity levels at 24, 48 and 72 dS/m salinity (Table 4). The highest reduction of Ca content at 24 dS/m was observed in species *D. didactyla* (24%), while least reduction was recorded in species *P. vaginatum* (6%). At highest salinity level (72 dS/m), Ca content of all species decreased but *C. dactylon* 'tifdwarf' and *C. dactylon* 'satiri' increased in compared to 48 dS/m. Shoot Ca contents varied inconsistently under different salt stress in species *C. dactylon* 'satiri' and *C. dactylon* 'tifdwarf'. There are several reports on considerable inhibition of Ca uptake under salinity (Netondo *et al*. 2004).

Table 4. The effect of different salinity levels on shoot Ca content of different turfgrass species (Values in the parentheses indicate times decrease compared to control).

Species	calcium content in mg /g, dry weight				LSD (0.05)
	Salinity levels (dS/m)				
	0	24	48	72	
C. dactylon 'satiri'	1.93 a (100)	1.58 b (82)	1.17 c (61)	1.43 d (74)	0.15
C. dactylon 'tifdwarf'	2.05 a (100)	1.76 a (86)	1.61 ab (79)	1.74 b (85)	0.28
Digitaria didactyla	1.48 a (100)	1.13 b (76)	0.79 c (53)	0.61 d (41)	0.06
Paspalum vaginatum	2.79 a (100)	2.62 b (94)	2.39 c (86)	2.07 d (74)	0.20
Zoysia japonica	2.17 a (100)	2.02 b (93)	1.75 c (81)	1.54 d (71)	0.17
Zoysia matrella	2.02 a (100)	1.85 b (92)	1.69 c (84)	1.40 c (69)	0.24

Means accompanied by common letters in rows are not significantly different at $P \leq 0.05$ by LSD test.

Shoot tissue Mg content decreased as salinity increased (Table 5). The highest Mg content in the shoot tissue was recorded at 24 dS/m salinity level and the lowest was at 72 dS/m. At 24 dS/m salinity, the highest Mg reduction was recorded in species *D. didactyla* (21%) and *C. dactylon* 'tifdwarf'; while least reduction were recorded in species *P. vaginatum* (3%) and *Z. japonica* (9%). Magnesium content at highest salinity level (72 dS/m), maximum reductions was found in species *D. didactyla* (56%) and *C. dactylon* 'tifdwarf' (53%) while least reduction were recorded in *P. vaginatum* (33%) *and Z. japonica* (41%). Dudeck and Peacock (1993) also reported that increasing Na affected Mg and K more than Ca tissue content in several turfgrasses they studied.

Table 5. The effect of different salinity levels on shoot Mg content of different turfgrass species (Values in the parentheses indicate times decrease compared to control).

Species	magnesium content in mg /g, dry weight				LSD (0.05)
	Salinity levels (dS/m)				
	0	24	48	72	
C. dactylon 'satiri'	3.60 a (100)	2.95 b (82)	2.10 c (58)	1.74 c (48)	0.37
C. dactylon 'tifdwarf'	3.18 a (100)	2.53 b (80)	1.91 c (60)	1.50 d (47)	0.21
Digitaria didactyla	3.01 a (100)	2.37 b (79)	1.70 c (57)	1.31 d (44)	0.17
Paspalum vaginatum	4.36 a (100)	4.21 b (97)	3.51 c (81)	2.91 d (67)	0.54
Zoysia japonica	3.07 a (100)	2.79 b (91)	2.42 c (79)	1.82 d (59)	0.21
Zoysia matrella	2.95 a (100)	2.59 b (88)	2.02 c (68)	1.46 d (50)	0.14

Means accompanied by common letters in rows are not significantly different at $P \leq 0.05$ by LSD test.

Conclusion

Increasing salinity resulted in enhanced Na uptake with the concomitant reduction of K, Ca, and Mg uptake in the shoot tissue. The lowest category of salt-tolerant species *D. didactyla* and *C. dactylon* 'tifdwarf' exhibited higher Na uptake and lower K, Ca, Mg uptake at high salinity compared to the salt-tolerant types (*P. vaginatum,* and *Z. japonica*). The shoot tissue content relationships of K, Mg, and Ca to increasing salinity provided insight into nutritional programs on salt-affected sites for these species. At the highest salinity level (72 dS/m), Ca content of all species decreased .*C .dactylon* 'satiri' and *C. dactylon* 'tifdwarf', in contrast, showed increased accumulation of Ca.

References

Ashraf M, Athar HR, Harris PJC, Kwon TR (2008) Some prospective strategies for improving crop salt tolerance. *Adv. Agron*. **97**, 45-110.

Carrow RN, Waddington DV, Rieke PE (2001) Turfgrass soil fertility and chemical problems: Assessment and management. (John Wiley & Sons, Hoboken, NJ).

Dudeck AE, Peacock CH (1993) Salinity effects on growth and nutrient uptake of selected warm season turf. *Int. Turfgrass Soc. Res. J.* 680-686.

Jacoby B (1999) Mechanism involved in salt tolerance of plants. In 'Handbook of plant and crop stress'. (Ed M Pessarakli) pp. 97-124. (Marcel Dekker, Inc., New York).

Netondo GW, Onyangoa JC, Beck E (2004) Sorghum and salinity, I: response of growth, water relations, and ion accumulation to NaCl salinity. *Crop Sci*. **44**, 797–805.

Qian YL, Wilhelm SJ, Marcum KB (2001) Comparative responses of two Kentucky bluegrass cultivars to salinity stress. *Crop Sci*. **41**, 1895–1900.

Rubinigg M, Posthumus F, Ferschke M, Elzenga JTM, Stulen I (2003) Effects of NaCl salinity on ^{15}N-nitreate f fluxes and specific root length in the halophyte *Plantago martima* L. *Plant Soil* **250**, 201–213.

SAS Institute (2006) 9.1.3 Procedures guide, second edition, Volumes 1- 4. Cary, NC: SAS Institute Inc.

Soil morphologic indicators of environmental hazards linked to cosmic airburst

Marie-Agnès Courty[A] and Michel Fedoroff[B]

[A]CNRS-UMR 7194. IPHES-ICREA, University Rovira i Virgili, Tarragona, Spain. Email courty@mnhn.fr
[B]Ecole Nationale Supérieure de Chimie de Paris, Paris, France. Email michel-fedoroff@enscp.fr

Abstract
Distinctive soil morphologies and fingerprints of cosmic airbursts are identified by comparing speculated impact-linked situations from various past records with three well known airburst events: the 1908 Tunguska event (Central Siberia), the Darwin glass layer (Western Tasmania) and the Henbury crater field (Central Australia). The signal of cosmic airbursts is isolated from the local background by high resolution observational and multi-analytical data. Two groups of anomalous debris are recognised: (G1) exogenic, metal rich organo-mineral components derived from terrestrial precursors, possibly tracing the collider; (G2) carbonaceous polymorphs formed by thermal cracking of G1volatile components that pulverised on the local vegetation. The association of G1 and G2 debris with a patchy pattern of fluffy ash and baked soil aggregates are characteristic of local ignition induced by the pyrogenic compounds of the heated collider while entering the atmosphere. Impact glass layers formed by pulverisation at the surface of the exogenic hot debris jet, but not from melting of the local soils. High resolution soil studies should contribute to further elucidate natural hazards linked to cosmic airburst, particularly firing effects due to local ignition by pyrogenic debris, acidifying risks from pulses of carbonaceous aerosols and long lasting contamination by resistant metals.

Key Words
Debris jet, Pulverisation, Ignition, Carbonaceous polymorphs, Metals, Terrestrial

Introduction

For long questioned as a reality of the Earth history, impact hazards generated by low-altitude airbursts from hypervelocity asteroid impacts are now speculated to occur frequently with damage on ecosystems and human populations (Osinski *et al.* 2008). However, the cataclysmic landscape with 4000 km^2 of devastated forest left by the 1908 Tunguska explosion in central Siberia remains so far the only observational data for calibrating processes linked to cosmic airbursts (Boslough and Crawford, 2008). The low range surface effects resulting from the blast waves and thermal radiation of the high-temperature jet of expanding gas would be more severe than for nuclear explosion of same yield. Larger cosmic airburst would generate a hot jet of vaporized projectile able to form the typical flow-textured impact glass by high temperature melting of the surface. In addition, airburst phenomena could produce small craters with impact melt fragments due to the impactor disruption at some significant altitude (Newsome and Boslough, 2008).
Here, the observational data of selected situations contribute to further explore the suite of processes generated at the soil surface by cosmic airbursts. We identify distinctive soil facies with their diagnostic tracers that are important to evaluate the range of environmental hazards linked to this specific phenomenon.

Materials and methods

Thirty bulk and undisturbed samples are studied from three situations that are representative of the main types of cosmic airburst for defining the specific morphology of the impact-linked soil facies and their associated markers in each case. The 1908 Tunguska layer identified by high resolution sampling on two peat sequences provides observational data to evaluate effects at the ground of the high-temperature fireball, assuming from previous studies total ablation of the collider (Svetsov, 1996). The scenario of surface melting is represented by the 400 km^2 strewnfield of Darwin glass in Western Tasmania with its distinctive layer just below the modern humic horizon of glass debris that were dated by Ar/Ar at ca. 0.8 Ma (Howard, 2008). The Henbury crater field in Central Australia provides data to study effects of airburst-linked cratering on the surrounding soils (Ding and Veblen, 2004).
We compare these reference sites of airburst events with anomalous soil morphologies that we speculated to be of impact origin due to the association of a patchy highly fired surface with exogenic debris formed of vesicular glass, partly melted and unmelted clasts (Courty *et al.,* 2008). The studied sites are located in the Middle-East, France and Peru. They comprise buried soils dated from the terminal Pleistocene, from ca. 4 kyr BP, and debris concentrations at the present soil surface. The spatial pattern and the microstratigraphic expression of the anomalous soil morphologies have been examined from widely exposed surfaces and serial trenches.
Undisturbed samples for thin section preparation were preferentially collected from the finest microstratigraphic records and from intact concentrations of debris including refitting fragments. Individual micro-strata and

patchy domains showing distinctive properties (colour, structure, debris concentrations) were sampled and subsequently water-sieved through the following meshes: >2 mm, 2-1 mm, 1-500 µm, 500-200 µm, 200-100 µm. Systematic examination of the residues under the binocular microscope was performed to isolate the anomalous signal from the local background. After gentle crushing and water-sieving, inclusions were extracted from the coarse debris and from the impact glass and compared with those of the host soil matrix. The preparation procedure was carried out with great care for controlling contamination by industrial products, especially abrasive paste or paper, nylon films, polymer resins, diamond paste or spray, detergent and metals. Observations were conducted in a microanalytical environmental scanning electron microscope (ESEM-EDS) on uncoated specimen. The possible contamination of polished specimens (studied using SEM-EDS and SEM-WDS) by diamond polishing and conductive coating was controlled by comparing to a raw slice. In situ mineralogical identification of individual particles down to 1 µg was performed by transmission X-ray diffraction. Representative particles were selected for Raman micro-spectrometry, isotope analysis (C, Cr, Fe, O, S), IR-GC-MS analysis, ICP-AES analysis and total chemical analyses. Dating by AMS C^{14} radiometric dating was performed.

Results

We identify similar unusual components that contrast from the respective local soil materials which can be separated in two groups according to their association with distinctive fractions of the host matrix: (G1) an exogenic assemblage of discrete particles occurring both as disseminated grains in the host matrix and as inclusions in the coarse debris and the true impact glass; (G2) components which do not occur as inclusions in debris and glass, often associated with plant debris that are common in the host matrix.

G1 comprises various types of metal rich mineral and organic components that are often associated with marine microfossils, fragmented, melted or intact (Figure 1a, 1b, 1c). Native metals (Fe, Fe-Cr, Fe-Cr-Ni, Cu-Zn, Cu-Zn-Ni, Pb, Pb-Cr, Al and Cr) are found as discrete spherules, ribbon-shape films and flakes and splashed droplets at the surface of the exogenic mineral grains. These components comprise various types of minerals, glass spherules and glassy flakes, fine-crystallized breccias and rock clasts of sedimentary and igneous origin. The organic components occur as discrete domains of amorphous carbon, often more graphitized, and commonly associated with hydrocarbons and aliphatic polymers. Pure carbonaceous grains are also encountered as translucent to blue blocky particles made of aliphatic polymers and grey, white or pale blue, crumby to ribbon-shape particles of polystyrene, and vesicular bitumen fragments. Soluble salts are encountered as either grains or neoformed crystals on the mineral grains, consisting of potassium and sodium chloride, barium, calcium and more rarely strontium sulphates. Individual spherules and spheroidal agglutinates of framboidal iron sulphide are common.

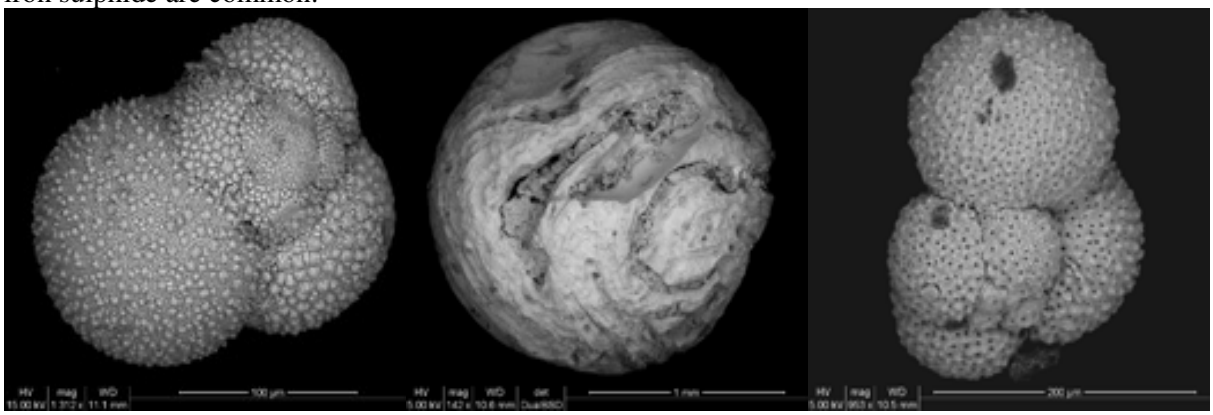

Figure 1. (a) 1908 Tunguska layer, intact foraminifera sprinkled by amorphous carbon. Darwin glass layer: (b) flow-textured glass spherule extracted from the fired soil surface: amorphous carbon and melted marine mud filling the cavities; (c) intact foraminifera sprinkled by amorphous carbon extracted from the Darwin impact glass.

We found commonly compound white carbonaceous fibres with nodules formed of fine quartz embedded within a green polymer glass sprinkled by native metals. Hexagonal crystals of sp^3 carbon have been identified by high resolution TEM in the green nodules and confirmed by XRD to be chaoite.

The G2 components consist of various carbonaceous polymorphs: translucent to coloured hollow fibres; hollow to vesicular carbonaceous spherules similar to those encountered in the ash residues produced from power plant stations; vesicular black vitreous grains; dull orange, brown, grey, green or pale blue, rubbery carbon grains. The plant debris occur as charred residues and translucent to slightly coloured intact fragments of stems and leaves. Charred residues with their distinctive plant morphology are often agglutinated by vitreous or microspheroidal graphitic carbon. Silicate cement showing partly melted coccolithic mud, Ca-sulphate and

sulphide, droplets of Ba-sulphate, zircons, euhedral crystals of rare earth phosphate, droplets of native metals of various composition (Ag, As, Au, Bi, Co, Hg, Ni, Pt, in addition to the ones listed above), are present at the surface and in the vesicles of the G2 components and on the plant debris. Lonsdaleite, i.e. detonation diamond, has been identified by Raman spectrometry in carbonaceous domains embedded in the silicate cement on the carbonaceous spherules.
Powdery white to brownish grey ash identified in the field as thin lenses or loose filling of subsurface root channels display high amount of carbonaceous fibres and spherules, finely mixed with calcinated plant fragments showing an internal carbonized part. The greater abundance of G1 components is observed in the ashy domains, occurring as individual particles ranging from sand to fine silt. In thin sections, the soil surface below the ash lenses often show an open packing of fragmented aggregates that locally have a baked-brick aspect. Ash lenses are also observed at the contact between the most intact concentrations of coarse vesicular debris or of the true impact glass and the underlying weakly baked soil surface. Careful control from these zones shows in the host soil matrix a size continuum from coarse sand to silt-sized debris of G1 components with angular shape.
Isotopic analyses performed on Fe, Pb, Cr, sulphur, oxygen and carbon are in agreement with a terrestrial origin of the precursor materials.
Radiocarbon ages of 2700 +/- 40 yr BP and 950 +/- 40 yr BP have been obtained respectively for vesicular carbon pine bark and pine wood extracted from the 1908 peat layer at Tunguska.
A radiocarbon age of 1820 +/- 40 yr BP has been obtained on charred wood extracted from the ashy burnt soil surface ***just underlying*** the layer of Darwin glass. Close to zero C^{14} activity has been obtained on the bitumen fragments and the vitreous graphitic carbon.

Discussion and perspectives
The observational and analytical data obtained on the three reference situations of cosmic airbursts help to elucidate the controversial aspects from earlier studies, and open an unexpected issue. In contrast with previous assumptions (Jehanno *et al.,* 1989), the terrestrial origin of the exotic components occurring in the 1908 Tunguska peat layer is unlikely to derive from later fall of industrial contaminants. The compositional coherence of the well sealed layer supports a synchronous fall of airborne debris resulting from a collider including components of terrestrial origin. The intimate incorporation of fine G1components into the charred and calcinated plant fragment (G2) suggests that the local vegetation was pulverised by a hot debris jet containing metal particles and carbonaceous volatiles. High amount of kerogen precursors (i.e. G1 organic components) in the debris jet would explain its pyrogenic efficiency on the local vegetation and the formation of the G2 organic components by thermal cracking. The two old ^{14}C values on the local charred pine express contamination by the dead carbon from the graphitic compounds at the time of burning. The lonsdaleite and the sp^3 hexagonal carbon incorporated into the pyrogenic debris would trace transformation by detonation of the graphitic carbon at the exact time of flash heating.
The similar observational and analytical data for the Darwin glass layer suggest that the airburst processes relate also to the explosive pulverisation of a hot debris jet from space of terrestrial origin. The sharp contact of the glass layer with the underlying fired soil surface, its compositional contrast from the local rocks, and especially the marine microfossils, preclude their formation from surface melting. The recent C^{14} age of the associated burnt layer is coherent with its position just below the weakly humified surface horizon and the nearly intact assemblage of glass debris. The active suite of glacial periods and soil forming episodes for 800 000 years on the Tasmanian dissected landscapes would have severely degraded a glass layer formed so long ago at the surface. This questions the exact significance of the 0.8 Ma Ar/Ar age of the Darwin glass.
Unfortunately, the over-picking of meteorite fragments and impact glass around the Henbury crater field, plus the scarce soil cover, have left nearly nothing for understanding the link between crater formation and airburst processes. However, the remaining patches of vesicular glass formed of exotic G1 debris of terrestrial origin suggest that the collider forming the crater field might have included a terrestrial component together with the fragments of the medium octahedrite IIIA iron meteorite.
The analogies between the anomalous soil morphologies from the various sites studied with the 1908 Tunguska layer and the Darwin glass layer support the hypothesis of their formation by airburst processes. The surprising similarity of the G1 components of terrestrial origin for situations of different ages and various contexts remains intriguing. Further investigations will help to test the hypothesis of occasional collisions between cosmic projectiles and terrestrial debris that were formerly launched to space by lithospheric cryptoexplosion (Morgan *et al*., 2004) Showers of terrestrial debris might not have been previously identified simply because only extra-terrestrial colliders are assumed so far to have bombarded the Earth. Because of their resemblance to kerogen-derived industrial products, the G2 components, might have been viewed as field or laboratory contamination,

or plant fibres. Their embedment by polymer films seems to have protected weakly resistant G1 components, especially the soluble salts from leaching, and the native metals from oxidation. The surprising resemblance of the powdery ashes with industrial ones from power plant station simply expresses similar combustion processes by pulsed air of fossil combustible. However, the original formation of polymers would express high volatile content in the colliding debris jet.

The patchy pattern of the ash lenses and fired domains shows that ignition by the pyrogenic compounds was erratic, depending upon production of volatiles in the hot debris jet.

These cosmic airbursts might also have ignited large scale wildfires in sensitive regions, just alike the disastrous ones initiated after drought of forested areas by lightning strikes or human incautiousness. Massive production of combusted biomass would probably dilute the original pyrogenic products, although the resistant vitreous carbon might be long lasting marker of the impact-linked ignition in contrast with the fragile charred fragments. The 1908 situation encountered in Central Siberia shows that there was not only surface devastation, but also thermal radiation from cosmic airburst which might have been lethal to many animal and human inhabitants, possibly inducing local mass killing of flocks. Finding for the distinctive fingerprints of the flash heating in the soil matrix embedding the bone accumulation would help to determine the exact cause of animal brutal death from past situations.

Future research will intend to trace effects in the soils that witnessed cosmic airbursts of the atmospheric perturbation caused by the carbonaceous aerosols, possibly acidification and precipitation increase due to cloud condensation nucleation processes. Detecting in past soils the long lasting contamination of the ecosystems by toxic metals that might have been critical for animal and human health is also a challenging issue.

Acknowledgments

Claude Peyron is warmly thanked for providing the Tunguska samples from the 1990 French-Russian expedition. The support of Ralph Bottrill for tracing the Darwin glass layer was greatly appreciated. We are grateful to Thierry Gé for conducting high resolution sampling on INRAP excavation from western France. We are indebted to many colleagues for their long lasting analytical support: Brigitte Deniaux for ESEM; Miguel Pernes and Francesc Guispert Guirardo for transmission XRD; Alan Brooker, Alex Crisci, Michel Mermoux and David Smith for Raman analyses; Kliti Greace and Paul Greenwood for GC-IR-MS analyses; Mark Thiemens for sulphur and oxygen isotopes; Jean-Louis Birck and Alex Shukolyukov for chromium isotopes; Franck Poitrasson for iron isotopes; Urs Schärer for lead isotopes; Ty Daulton and Michael Walls for TEM and EELS; Franck Bassinot, Elsa Cortijo, Xavier Crosta, Jacques Giraux et Guiseppe Cortese for identification of marine microfossils.

References

Boslough MBE, Crawford DA (2008) Low-altitude airbursts and the impact threat. *International Journal of Impact Engineering* **35**, 1441–1448.

Courty MA, Crisci A, Fedoroff N, Greenwood P, Grice K, Mermoux M, Smith DC, Thiemens MH (2008) Regional manifestation of the widespread disruption of soil-landscapes by the 4 kyr BP impact-linked dust- event using pedo-sedimentary micro-fabrics. In 'New Trends in Soil Micromorphology'. (Eds S Kapur, A Memut, G Stoops) pp. 211-236. (Berlin: Springer).

Ding Y, Veblen DR (2004) Impactite from Henbury, Australia. *American Mineralogist* **89**, 961–968.

Howard KT (2008) Geochemistry of Darwin glass and target rocks from Darwin Crater, Tasmania,. Australia. *Meteoritics and Planetary Science* **43**, 1-2.

Jehanno C, Boclet D, Danon J, Robin E, Rocchia R (1989) Analytical study of spherules from the site of the Tunguska Explosion. *Comptes Rendus Académie des Sciences Paris* **297**, Serie II, 0478-0484.

Morgan JP, Reston TJ, Ranero CR (2004) Contemporaneous mass extinctions, continental flood basalts, and 'impact signals': are mantle plume-induced lithospheric gas explosions the causal link? *Earth and Planetary Science Letters* **217**, 263-284.

Newsome HE Boslough MBE (2008) Impact Melt Formation by Low-Altitude Airburst, Evidence from Small Terrestrial Craters and Numerical Modeling. *Lunar and Planetary Science* XXXIX **1391**, 1460.

Osinski G, Kienewicz J, Smith JR, Boslough MBE, Eccleston M, Schwarcz HP, Kliendienst MR, Haldelmann AFC, Chucher CS (2008) The Dakhleh Glass: Product of an impact airburst or cratering event in the Western Desert of Egypt? *Meteoritics and Planetary Science* **43**, 12, 2089–2107.

Svetsov VV (1996) Total ablation of the debris from the 1908 Tunguska explosion. *Nature* **383**, 697–9.

Technosols of Hope Bay, Antarctic Peninsula: Century-old man made soils on Former Ornithogenic Environment

Carlos E. G. R. Schaefer[A]; Thiago T. C. Pereira[A]; Felipe N.B.Simas[A], Marcelo Braga Bueno Guerra[B]; João C. Ker[A], Ivan C. Carreiro Almeida[A]; Edenir R. Pereira-Filho[B]

[A]Universidade Federal de Viçosa, UFV, Soil Science Department, Email carlos.schaefer@ufv.br
[B]Universidade Federal de São Carlos, UFSCar, Chemistry Department

Abstract
Technosols are anthopogenic soils that may be strongly impacted by heavy-metal deposition, which have not yet been described in Antarctica. In this paper, we present the chemical and physical study of what is supposedly the oldest man-made soil from Antartic Peninsula, developed in the vicinity of Trinity House and Nordenskjold Hut at Hope Bay. The soil morphology and chemistry indicates a former ornithogenic site (penguin rookery) further subjected to human disturbance, following exploration since 1903. We detected very high amounts of exchangeable Zn, Fe, Mn, Cu, all consistent with the human impacts and strong contamination. Also, the total contents of heavy metals such as Cd, Cu, Ni, Pb and Zn are extremely high. Strong positive correlation between the total concentrations of Cd, Cu, Mn, Ni, Pb and Zn indicates a similar source of pollution. These soils may represent the oldest Technosol in the Antarctic Continent.

Introduction
The first report of human presence in Hope Bay (Antartctic Peninsula) date back to 1903, when J. Gunnar Andersson, a member of the Swedish expedition to the south pole (1901-1904), under the leadership of Otto Nordenskjöld, carried out the first exploration and mapping. Well-preserved ruins of the stone hut built by the swedish group can be seen at the harbour entrance. The United Kingdom first established at Hope Bay in 1945 (the so-called Base D – built as part of "Tabarin Operation"). The British station remained operational until 1964, being transferred to Uruguai in 1997. In 1951, Argentina also established an Army station in the region (Esperanza), with permanent operation to the present day. In the same area, remains of a former British Base (Trinity House), which burnt down in 1948, are situated 300 metres to the northeast of the Uruguayan base. The population of breeding birds of Hope Bay is well studied, and a large Adélie penguin (*Pygoscelis adeliae*) colony, numbering around 125,000 pairs, is situated about the same area (Woehler 1993). Soil morphological aspects indicating strong ornithogenic influence suggest that the extension of the penguin rookery was much larger prior to permanent human settlement. Other birds breeding at Hope Bay include gentoo penguins (*Pygoscelis papua*), brown skua (*Catharacta loennbergi*), Antarctic tern (*Sterna vittata*), Wilson's storm petrel (*Oceanites oceanicus*), kelp gull (*Larus dominicanus*), and sheathbill (*Chionis alba*).

The aim of this work was to study the occurrence and chemical composition of unusual Antartic soils under strong anthropogenic influence at the vicinity of Trinity House at Hope Bay, and relating chemical and morphological changes with the history of occupation of this area, as this possibly represents one of the oldest memories of anthropogenic impact of the Antarctic Continent. We hypothesized that these soils may represent Technosols (WRB, 2006).

The last version of the World Reference Base for Soil Resources (IUSS Working Group WRB, 2006) developed appropriate taxa (Anthrosols and Technosols) for soils in urban/industrial areas (landfills, farming, earth movement, and heavy metal contamination), and agricultural areas (erosion, ripping, and land leveling).

Methods
Soil profiles at selected anthopogenic sites were dug and collected at the vicinity of the ruins of the British depot of Trinity House, which burned down to complete destruction, leaving a widespread mantle of debris which was subjected to further pedological changes under a cold polar climate. This anthropic action left varied materials, such as semi-carbonized wood, bone, charcoal, bricks, charred organic materials, metallic materials, concrete, distributed at depths between 5 cm down to 30-40 cm.
The chemical extraction of nutrients and metals followed the procedure of Embrapa (1997): we determined pH in water; Mehlich 1-extractable amounts of P, Na^+, K^+, Zn, Fe, Mn and Cu; Available Ca^{2+}, Mg^{2+} and exchangeable Al^{3+} with KCl 1 mol L^{-1}. Total Organic carbon was estimated by wet combustion by the method of Yeomans and Bremner (1988).

Aqua regia extraction (pseudototal content) was done according to the German Norm (DIN 38414-S7)[1]. Three hundred milligram of dried soil samples, in triplicate, was weighed to digestor blocks tubes and 3 mL of aqua regia were added. The mixture was allow to stand at room temperature overnight. Then the tubes were transferred for a digestor block and a warming step of 3 hours at 120 ºC was done using a reflux apparatus. Finally the extracts were transferred to previously decontaminated tubes and the final volume was completed to 10 mL. In order to assess the bioavailable fraction of metals in these soil samples, a extraction with DTPA were performed. The DTPA extraction solution was prepared with 0.005 mol L^{-1} of Diethylenetriamine-pentaacetic acid (DTPA), 0.01 mol L^{-1} $CaCl_2$ buffered at pH=7.30 with triethanolamine[2]. One gram of each soil sample, in triplicate, were extracted with 5 mL of DTPA solution in a horizontal shaker end-over-end (Barnsteady, Iowa, USA) by 2 h. The supernatant was separated by centrifugation and it was transferred to previously decontaminated flasks. Spectrometric determinations of the elements Cd, Cr, Cu, Mn, Ni, Pb and Zn in the aqua regia and DTPA extracts were done using flame atomic absorption spectrometry. The accuracy of the aqua regia extraction was verified by the use of the certified reference material BCR 146 R (Sewage Sludge from Industrial Origin).

Results

These anthropogenic soils of Hope Bay showed mean values of Mehlich-1 extractable P of 996 mg dm^{-3} (HB1) and 679 mg dm^{-3} (HB2) (Table 1), and thus classified as strongly ornithogenic, according to criteria proposed by Simas et al. (2007). The parent materials of the Hope Bay Formation are generally chemically poor in bases and P (siliclastic tubidites and sandstones), indicating that the abnormal P values are related to a former penguin rookery, which was either went extinct or was forced to move away from the direct human influence following the swedish and british occupations in early XX century. In fact, slaughtering of penguins was described by O. Nordenskjöld at the 1903 season (SCAR, 2002), a fact which was possibly repeated in the following years of occupation, greatly reducing the original rookery.

Very high amounts of exchangeable Zn, Fe, Mn, Cu are consistent with the human impacts and strong contamination of the local soil following human occupation. It is also possible that the contamination and further pedogenesis and cryoturbation led to a larger extent of soil pollution, as indicated by morphological observation at the field. According to critical values for the Brazilian Law (Cetesb 2005), such Zn concentration of 987 mg dm^{-3} (surface), and extractable Cu of 101 mg dm^{-3} (subsurface), found in HB1 profile indicate urgent need for intervention, in view of imminent, direct or indirect, risk to human health. In this case, particular attention should be given to water pumping at nearby lake Boekella, used for the Argentinian Base. Furthermore, the pseudototal contents of heavy metals such as Cd, Cu, Ni, Pb and Zn are extremely high. For the most impacted sites (table 2), pseudototal levels of these elements were almost 36, 35, 26, 270 and 87times higher than the prevention value for soil quality prescribed by the CETESB, respectively. Regarding the bioavailable contents, great environmental concern was raised, especially the high Pb concentration in the more labile fraction, reaching 2094 mg kg^{-1}. A matrix correlation (table 3) was constructed using the pseudototal and bioavailable concentrations of the elements. Positive correlations were obtained between pseudototal and bioavailable concentration of each element, showing a good selectivity of the DTPA extractant. Nevertheless, the most important information obtained with that matrix was a good correlation between the pseudototal concentrations of Cd, Cu, Mn, Ni, Pb and Zn, which indicates a similar source of pollution.

Lower TOC are the result of poor vegetation development and little vestiges of the original penguin guano deposition, which was further mineralized and leached following abandonment. Present-day vegetation is restricted to a few crostose lichens (Acarospora) and matts of *Prasiola Crispa* (algae).

In the two soils, anthrosolization dominates the soil forming process, being man-made soils. They can be classified as Technosols, formed under the influence of deposited debris, without further direct anthropic interventions, nearly a century-old. Strong horizonation and redistribution of metals are indicating that cryoturbation under a polar climate did not prevent pedogenesis and sparse colonization of lower plants. Results also indicate an ability of these Antarctic Technosols to retain nutrients and heavy metals.

Conclusions

The soil pedons HB1 and HB2, are both anthropogenic, and previously developed under strong ornithogenesis before human arrival in 1903. At that time, the penguin rookery at Hope Bay was much larger than at present, having its size reduced following permanent settlement in this area.
Tentatively, these soils can be classified as Gelic, ornithogenic Anthosols. Very high exchangeable,

pseudototal and bioavailable amounts of heavy metals indicate contamination and disturbance, especially by debris left by the burning of the British Base Trinity House, close to the studied soil. This illustrates that the Hope Bay area needs to establish a permanent protected area in the remaining penguin rookery, allowing a long term recovery of the original landscape.

Table 1. Chemical characterstics of Anthosols

Hor.	Prof.	pH		Ca^{2+}	Mg^{2+}	K^+	Na^+	Al^{3+}	MO	P	P_{rem}	Zn	Fe	Mn	Cu
	(cm)	H_2O	KCl	----------$cmol_c\ dm^{-3}$----------					$dag\ kg^{-1}$	$mg\ dm^{-3}$	$mg\ L^{-1}$	----------$mg\ dm^{-3}$----------			
HB1 - Gelic Ornithogenic Anthrosol															
A	0-8	7,36	7,38	4,56	0,97	0,30	1,43	0,00	3,23	1156,10	26,00	987,00	302,30	200,40	94,20
AC	8-12	6,98	6,12	4,96	1,26	0,78	1,52	0,00	1,03	1921,50	33,00	184,50	576,20	61,80	101,90
C2	12-27	5,11	3,60	1,16	0,63	0,85	0,56	1,05	0,52	480,50	48,80	14,49	1020,20	5,90	13,98
C3	27-53	4,87	3,33	0,55	0,51	0,51	0,32	0,86	0,39	427,20	56,60	3,92	482,70	2,20	4,76
HB2 -Gelic Ornithogenic Anthrosol															
A	0-18	6,04	5,93	1,88	1,08	0,20	0,53	0,00	2,91	718,00	50,40	42,40	875,40	58,30	22,00
C1	18-27	4,85	3,86	1,45	0,91	0,18	0,39	0,76	1,42	865,00	51,20	144,00	604,80	19,80	8,08
C2	27-60	4,81	3,45	1,22	0,81	0,15	0,23	2,00	0,78	454,70	39,50	11,51	628,70	6,90	4,06

Table 2. Pseudototal and bioavailable contents of Cd, Cr, Cu, Mn, Ni, Pb and Zn of the soil samples

Samples	Cd ($mg\ kg^{-1}$)		Cr ($mg\ kg^{-1}$)		Cu ($mg\ kg^{-1}$)		Mn ($mg\ kg^{-1}$)		Ni ($mg\ kg^{-1}$)		Pb ($mg\ kg^{-1}$)		Zn ($mg\ kg^{-1}$)	
	pseudo	Bio	pseudo	bio	pseudo	bio	pseudo	bio	pseudo	bio	pseudo	bio	pseudo	bio
A1	< LD	< LD	34	< LD	105	0.48	195	6.0	10	< LD	129	< LD	405	17
A2	7.2	0.49	225	< LD	159	1.0	326	12	106	2.8	437	22	3484	460
A3	4.1	0.46	60	< LD	580	2.5	315	9.4	18	0.99	250	6.2	1554	84
Gerador	< LD	< LD	46	< LD	104	0.29	128	3.8	7.4	< LD	184	< LD	134	6.0
50 m	< LD	< LD	74	< LD	150	0.62	73	1.7	4.2	< LD	250	7.8	151	6.0
PERR	< LD	< LD	35	< LD	195	0.49	202	5.6	12	1.22	103	< LD	263	10
MOTOR	47	1.9	90	< LD	2081	1.7	3197	5.4	336	1.69	18605	1817	5225	301
CONST	44	2.0	99	< LD	1836	3.2	2661	4.9	278	1.57	19381	2094	4422	242

Table 3. Correlation matrix

	Cd b	Ni b	Pb b	Cu b	Mn b	Zn b	Cd ps	Ni ps	Pb ps	Cu ps	Mn ps	Zn ps	Cr ps
Cd b	-	0,39	0,97	0,96	0,01	0,60	0,99	0,98	0,98	0,98	0,98	0,92	0,27
Ni b	-	-	0,26	0,23	0,71	0,95	0,36	0,49	0,26	0,24	0,30	0,69	0,93
Pb b	-	-	-	0,96	-0,18	0,46	0,98	0,95	0,99	0,97	0.98	0,83	0,12
Cu b	-	-	-	-	-0,19	0,44	0,98	0,95	0,98	0,99	0,99	0,83	0,08
Mn b	-	-	-	-	-	0,65	-0,07	0,03	-0,18	-0,11	-0,12	0,33	0,67
Zn b	-	-	-	-	-	-	0,57	0,68	0,47	0,47	0,51	0,86	0.90
Cd ps	-	-	-	-	-	-	-	0,99	0,99	0,98	0,99	0,90	0,22
Ni ps	-	-	-	-	-	-	-	-	0,96	0,95	0,98	0,95	0,34
Pb ps	-	-	-	-	-	-	-	-	-	0,98	0,99	0,84	0,13
Cu ps	-	-	-	-	-	-	-	-	-	-	0,99	0,85	0,09
Mn ps	-	-	-	-	-	-	-	-	-	-	-	0,87	0,14
Zn ps	-	-	-	-	-	-	-	-	-	-	-	-	0,58
Cr ps	-	-	-	-	-	-	-	-	-	-	-	-	-

Acknowledgements

Financial support was provided by Brazilian agencies CNPq (INCT Criosfera and IPY project) and FAPEMIG, and logistical support from the Brazilian Antartic Program during the International Polar Year.

References

Cetesb. Decisão da Diretoria n 195/2005. (2005) Aprovação dos valores orientadores para solos e águas subterrâneas no Estado de São Paulo, CETESB, São Paulo.

DIN 38 414 Part 7 (1983) German standard methods for the examination of water, waste water and sludge, sludge and sediment (Group S), Digestion using aqua regia for the subsequent determination of the acid-soluble portion of metals (S7).

Embrapa (1997) Manual de Métodos de Análises de Solos, 2nd edition. Rio de Janeiro.

Lindsay WL, Norvell WA (1978) *Soil Sci. Soc. Am. J.,* **42**, 421-428.

Woehler EJ (1993) The distribution and abundance of Antartic and Subantarctic penguins. Cambridge: Scientific Committee on Antarctic Research.

WRB (2006) World Reference Base for Soil Resources. World Soil Resources Report 84, 2006. FAO, Rome, IT, EU.

Yeomans JC, Bremer JM (1988) A rapid and precise method for routine determination of organic carbon in soil. *Communications in Soil Science and Plant Anal*. **19**, 1467-1476.

Transformation of vertical texture-contrasted soils due to accelerated erosion in young glacial landscapes, North-Eastern Poland

Marcin Świtoniak

Department of Soil Science, Institute of Geography, Faculty of Biology and Earth Sciences, Nicolaus Copernicus University, Torun, Email Poland, swit@umk.pl

Abstract
The purpose of the present paper is to elucidate the influence of accelerated soil erosion on vertical texture contrasted soils (VTC-s) in young glacial landscapes of North-Eastern Poland. To solve the problem, a comparison of non eroded forest reference VTC pedons with arable soil has been made. On the basis of the results, five classes of VTC-soil truncation have been distinguished. According to the identified degrees of truncation, maps of soil cover transformation, caused by accelerated erosion, were generated and overlapped on Digital Elevation Models (DEMs). The widespread occurence of strongly and completely eroded investigated soils provides intense anthropical pressure on soil cover in the agriculture areas of North-Eastern Poland.

Key Words
Accelerated erosion, soil truncation, vertical texture contrast, slope processes

Introduction

Soil erosion is a natural phenomenon and has occurred throughout the geological history. Human activities have increased erosion rates. This human influenced process is termed accelerated erosion. Land use conversion modified soil morphological properties along the slope due to soil material redistribution (Papendick and Miller, 1977; De Alba *et al*., 2004; Marcinek and Komisarek, 2004). Surface soil horizons loss (truncation) occurs on convex parts of slopes and colluvial material deposition takes place on concave areas. Soil erosion is one of the key threats to soil in Poland. Some authors estimated that almost 30% of the total area of the country is considerably degraded by this process (Józefaciuk and Józefaciuk, 1992). Accelerated soil erosion in the hilly young glacial agricultural landscapes of North-Eastern Poland is a particulary important problem (Uggla *et al*., 1968). Since the end of the 10th century, this area is strongly influenced by anthropic pressure and has suffered a heavy soil erosion, aggravated by agriculture and deforestation (Sinkiewicz, 1998). The strongest transformations occur in regard to arable soils developed on ground moraine deposits in hummocky moraine plateau landscapes. A common feature of untruncated soils in this area is the presence of a coarse-over-fine vertical texture-contrast (VTC) with an abrupt textural change. The VTC is inherited from the parent material: a sandy ablation and fluvioglacial layer (thickness about tenths of centimeters) covering the more heavy lodgment till (Niewiarowski 1986; Niewiarowski, Wysota, 1986). In most primary pedons, geological VTC was increased by an eluviation-illuviation (*lessivage*) process. In some cases, the features characteristic for clay illuviation were not present. A morphological similarity (despite of differences in pedogenesis) and complicated genetic horizons sequences of forest, non truncated VTC-soils can be useful as reference pedons to a determination degree of arable soils transformation by erosion. Soil profile truncation and accretion have been used by other authors to estimate the intensity of erosion in rural areas (Lowrance *et al*., 1988; Phillips *et al*., 1999). In the studied area the problem has not received sufficient attention yet (Sinkiewicz, 1998). The aim of the present paper is to define several classes of VTC-soils truncation and to test their applicability in the estimation of soil cover erosion spatial range.

Methods

The soils of two study sites (1 km square each site) in Brodnica Lake District, North-Eastern Poland (Figure 1) were mapped in detail (soil maps were drawn on a scale 1:10,000) . The relief of the studied area is typical for hummocky moraine plateau landscapes. Twenty profiles developed on ground moraine deposits were described and sampled. The first site (A) represents the mixed forest area and a natural stage of a soil cover development. The second site (B) is a rural area with strong modifications of soils due to erosion. Twelve pedons were located under mixed forests (Site A), and eight were situated in arable areas (Site B). Apart from soil pits, 375 augerholes, 200 cm deep, were made. Two Digital Elevation Models (DEM) of the study sites were derived. DEMs were constructed at 10 m resolution by interpolation from the spot heights and digitised contours with 1.25 m interval of the 1:10,000 topographic map. Interpolation was fitted using a kriging method, incorporated

in the Grid tool of SURFER 8 (Golden Software, Inc. 1999).
The samples were taken from selected soil horizons. Standard soil analyses were performed according to the methods as follows (Bednarek *et al*., 2004) :
- Organic carbon content – by sample oxidation in the mixture of $K_2Cr_2O_7$ and H_2SO_4;
- Total nitrogen content – Kjeldahl method;
- $CaCO_3$ content – Scheibler volumetric method;
- Grain size distribution – by pipette and sieve method;
- pH of soil-to-solution ratio of 1:2,5 using 1M KCl and H_2O as the suspension medium;
- Hydrolythic acidity by Kappen method;
- Exchangeable Cations content by leaching with 1M ammonium acetate;
- Colour has been described according to Munsell (Munsell Soil Colour Charts 2000).

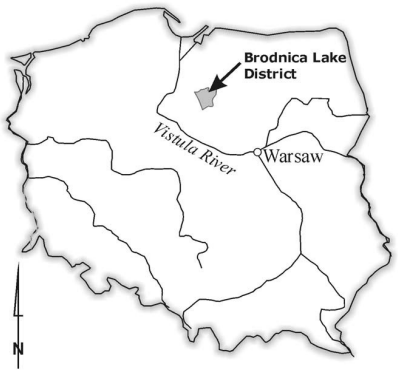

Figure 1. Location of the study area within Poland

For micromorphological investigations 14 samples with undisturbed structure were taken according to Mroczek (2001). Thin sections (55x75 mm) were prepared according to Lee and Kemp (1992). Description of micromorphological features was made according to Mroczek (2008), based on nomenclature created by Bullock *et al*. (1985) with Stoops (2003) modifications. Thin section and their description were made by Przemysław Mroczek from Maria-Curie Sklodowska University in Lublin, Poland. The soils were classified according to WRB (IUSS-FAO 2006). The symbols of soil horizons are given after Guidelines for Soil Description (FAO 2006).

Results
Investigated soils represented whole spectrum of truncation caused by accelerated erosion. Five classes of VTC-soils truncation have been distinguished (Figure 2):
1) Non eroded VTC-soils
Pedons located under mixed forest had fully developed sequences of horizons. Depending on the degree of pedogenesis (Świtoniak 2006, 2008) they were divided into two main groups: Luvisols (VTC-soils with argic horizon) and Umbrisols or Arenosols (VTC-soils without argic horizon). All non-eroded pedons had abrupt textural change at a depth of tenths of centimeters. The upper sandy layer contained, directly below the A horizon, a visible "minimum B-horizon". The transformation of soil material into a Bw horizon is evident as brownish staining caused by the accumulation in situ of iron sesquioxides. A sandy E horizon (Luvisols) or parent material (Umbrisols and Arenosols) exists between Bw horizons and the abrupt textural change boundary.
2) *Slightly eroded VTC-soils*
Soils without Bw horizons. In most non-eroded forest soils Bw horizons thickness was deeper than the average plowing depth in the arable areas. The lack of Bw horizons in arable VTC-soils should be attributed to shallowing due to erosion.
3) *Moderately eroded VTC-soils*
Increased erosion led to truncated E (Luvisols) or C (Arensols, Umbrisols) horizons. Ap horizons overlay directly Bt horizons. The abrupt textural change takes place at 20-30 centimeters and contemporaneously delimits the Ap horizons lower boundary. Surface humus horizons contain sandy material from primarily E or C horizons which were completely mixed by plowing with Ap horizons.
4) *Strongly eroded VTC-soils*
The material from the eluvial horizons of Luvisols was entirely removed. Surface horizons include illuvial material from argic horizons (ApBt). At this stage of truncation, luvisols have a morphology identical to

cambisols (A-B-C sequences) and become texturally homogeneous. The illuvial character of the B horizons was established using micromorphology. A basic criterion used to distinguish the argic horizon was the presence of illuvial forms of clay concentration. For VTC-soils without the argic horizons this class of truncation can not be differentiated because these pedons do not have suitable diagnostic properties for an argic horizon.

5) *Completely eroded VTC-soils*

All diagnostic horizons and characteristical properties of VTC-soils were entirely truncated. Pedons represent ACp-C or ACkp-Ck morphology with no other diagnostic horizon than an ochric surface horizon. This minimal development permits to classify these soils only as Regosols.

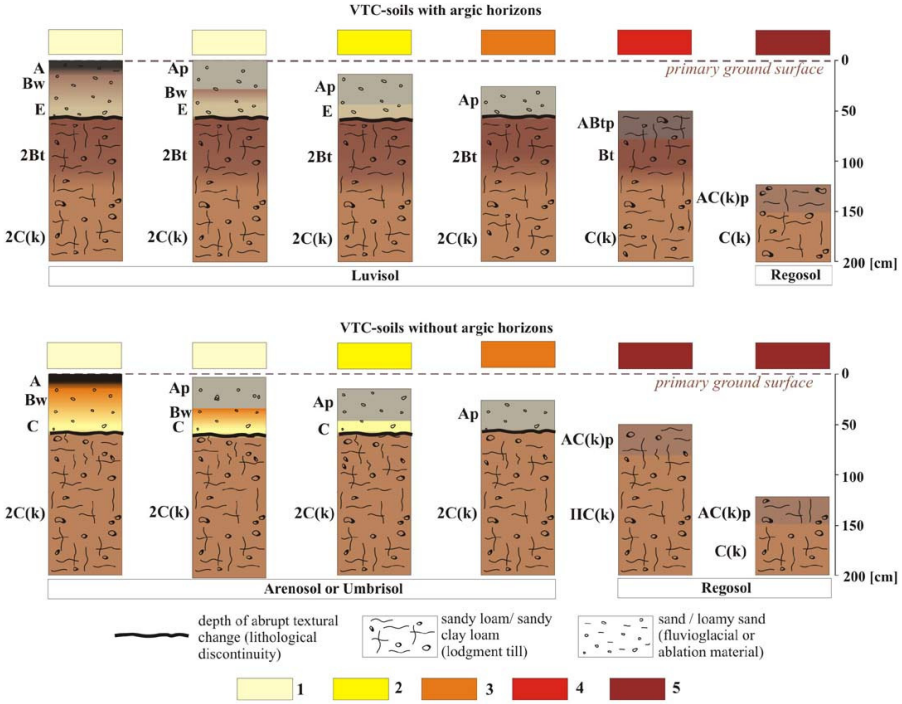

Figure 2. Classes of VTC-soils truncation: 1 – non eroded, 2 – slight, 3 – moderate, 4 – strong, 5 – complete

According to the identified degrees of truncation, maps of soil cover transformation caused by accelerated erosion were generated and overlapped on DEMs (Figure 3).

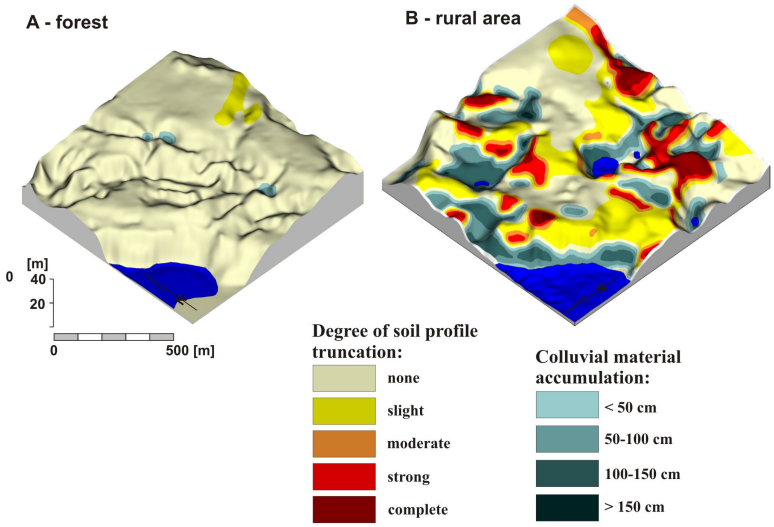

Figure 3. Soil cover transformation due to accelerated erosion on the two study sites.

Conclusion

The distinguished successional stages of VTC-soils truncation can be used as a suitable indicator of accelerated erosion range and intensity in young glacial landscapes. The widespread occurence of strongly and completely eroded investigated soils provides intense anthropic pressure on soil cover in the agriculture areas of North-

Eastern Poland. Truncation of pedons with abrupt textural change due to the slope processes lead to disappearance of vertical textural contrasts and the formation of new soil units. The insignificant degree of erosive alteration and the range of soil cover transformation in forests areas prove that it is ananthropogenic character.

Acknowledgments
This work was supported by Ministry of Science and Higher Education, Poland. Research grant No. N N305 283337.

References

Bednarek R, Dziadowiec H, Pokojska U, Prusinkiewicz Z (2004) Ecopedological studies. Polish Scientific Publisher PWN. Warsaw (in Polish).

Bullock S, Fedoroff N, Jongerius A, Stoops G, Turisna T (1985) Handbook for Soil Thin Section Description. Waine Research Publ. Wolverhampton. England.

De Alba S, Lindstrom M, Schumacher TE, Malo DD (2004) Soil landscape evolution due to soil redistribution by tillage: a new conceptual model of soil catena evolution in agricultural landscapes. *Catena* **58**, 77-100.

Golden Software, Inc. (1999) Surfer. User's Guide. Contouring and 3D Surface Mapping for Scientists and Engineers.

FAO (2006) Guidelines for Soil Description. Fourth edition. FAO. Rome.

IUSS Working Group –FAO (2006) WRB-World Reference Base for soil resources 2006. World Soil Resources Report No. 103. FAO. Rome.

Józefaciuk A, Józefaciuk Cz (1992) Struktura zagrożenia erozją wodną fizjograficznych krain Polski. *Pamiętnik Puławski* **101**, 23-49.

Lee J, Kemp RA (1992) Thin section of unconsolidated sediments and soils: a recipe. Thin Section Laboratory, Sediment Analysis suite. Geography Department. Royal Holloway. University of London. Egham.

Lowrance R, McIntire S, Lance C (1988) Erosion and deposition in a field estimated using cesium-137 activity. *Journal of Soil and Water Conservation* **43**, 195-199.

Marcinek J, Komisarek J (2004) Antropogeniczne przekształcenia gleb Pojezierza Poznańskiego na skutek intensywnego użytkowania rolniczego. AR. Poznań.

Mroczek P (2001) Micromorphology of clastic deposits and soils. Subject, application and choosen analytic methods. *Czas. Geogr.* **72(2)**, 211-229 (in Polish with English summary).

Mroczek P (2008) The Paleogeographical Interpretation of Micromorphological Features of the Neopeistocene Loess-Paleosol Sequences. UMCS. Lublin.

Munsell Soil Colour Charts (2000) GreagMacbeth. New Windsor.

Niewiarowski W (1986) Morphogenesis of the Brodnica outwash on the background of other glacial landforms of Brodnica Lake District. *AUNC. Geography* **19(60)**, 3-30 (in Polish with English summary).

Niewiarowski W, Wysota W (1986) Poziomy wysoczyznowe Wysoczyzny Brodnickiej. *AUNC. Geography* **19(60)**, 39-46.

Papendick RI, Miller DE (1977) Conservation tillage in the Pacific Northwest. *Journal of Soil and Water Conservation* **32**, 49-56.

Phillips JD, Slattery M, Gares PA (1999) Truncation and accretion of soil profiles on coastal plaincroplands: implications for sediment redistribution. *Geomorphology* **28**, 119-140.

Sinkiewicz M (1998). Rozwój denudacji antropogenicznej w środkowej części Polski północnej. UMK. Toruń.

Stoops G (2003) Guidelines for Analysis and Description of Soil and Regolith Thin Sections. SSSA. Madison Wisconsin. USA.

Świtoniak M (2006) Different pedogenesis conditioned by lithology of texture-contrast soils in Brodnica Lake District. In 'Ideas and practical universalism of geography' (Eds. P Gierszewski, M. Karasiewicz). Geographical documentation. **32,** 278-285 (in Polish).

Świtoniak M (2008) Classification of young glacial soils with vertical texture-contrast using WRB system. *Agrochimija i Gruntoznawstwo: Charkiw* **69**, 96-101.

Uggla H, Mirowski Z, Grabarczyk S, Nożyński A, Rytelewski J, Solarski H (1968) Proces erozji wodnej w terenach pagórkowatych północno-wschodniej części Polski. *Rocz. Glebozn*. **18(2),** 415-446.